JEM Journal of Experimental Medicine

ARTICLE

A Fas-4-1BB fusion protein converts a death to a pro-survival signal and enhances T cell therapy

Shannon K. Oda[1], Kristin G. Anderson[1], Pranali Ravikumar[1], Patrick Bonson[1], Nicolas M. Garcia[1], Cody M. Jenkins[1], Summer Zhuang[1], Andrew W. Daman[1], Edison Y. Chiu[1], Breanna M. Bates[1], and Philip D. Greenberg[1,2]

Adoptive T cell therapy (ACT) with genetically modified T cells has shown impressive results against some hematologic cancers, but efficacy in solid tumors can be limited by restrictive tumor microenvironments (TMEs). For example, Fas ligand is commonly overexpressed in TMEs and induces apoptosis in tumor-infiltrating, Fas receptor–positive lymphocytes. We engineered immunomodulatory fusion proteins (IFPs) to enhance ACT efficacy, combining an inhibitory receptor ectodomain with a costimulatory endodomain to convert negative into positive signals. We developed a Fas-4-1BB IFP that replaces the Fas intracellular tail with costimulatory 4-1BB. Fas-4-1BB IFP-engineered murine T cells exhibited increased pro-survival signaling, proliferation, antitumor function, and altered metabolism in vitro. In vivo, Fas-4-1BB ACT eradicated leukemia and significantly improved survival in the aggressive KPC pancreatic cancer model. Fas-4-1BB IFP expression also enhanced primary human T cell function in vitro. Thus, Fas-4-1BB IFP expression is a novel strategy to improve multiple T cell functions and enhance ACT against solid tumors and hematologic malignancies.

Introduction

Adoptive T cell therapy (ACT) is a promising treatment option that uses immune cells to find and destroy cancer. This approach has been FDA approved for patients with some B cell malignancies, but efficacy against solid tumors has been limited, in part due to inhibitory tumor microenvironments (TMEs) that can impede antitumor T cell function (Martinez and Moon, 2019). Multiple obstacles have been described, including inadequate tumor infiltration by T cells, up-regulated inhibitory and death receptor ligands, and limited availability of metabolic substrates (Anderson et al., 2017; Binnewies et al., 2018).

Although chimeric antigen receptors (CARs) can target surface proteins, TCRs can also target intracellular proteins and are highly sensitive to low abundance antigens. We have shown in clinical trials that TCR-engineered T cell (TCR-T) therapy can safely prevent relapse (Chapuis et al., 2019), but T cells often become dysfunctional after transfer and can fail to persist (Stromnes et al., 2015; Thommen and Schumacher, 2018). We therefore pursued novel T cell engineering to boost T cell function with immunomodulatory fusion proteins (IFPs) that combine an inhibitory ectodomain with a costimulatory endodomain. Like current checkpoint blockade therapies, this approach can abrogate an inhibitory signal but additionally provides a costimulatory signal that is often absent in the TME. Moreover, these altered signals are cell intrinsic, delivered to only the T cells concurrently engineered to be tumor specific, thereby avoiding systemic T cell activation. We previously showed that targeting the CD200 inhibitory ligand with a CD200R-CD28 IFP produced a strong costimulatory signal and improved T cell function and ACT efficacy in a mouse model of leukemia (Oda et al., 2017). Similar strategies have been described with PD-1–CD28 IFPs, suggesting that this strategy could broadly overcome inhibitory signals (Ankri et al., 2013; Kobold et al., 2015; Liu et al., 2016; Prosser et al., 2012; Schlenker et al., 2017).

To generate an IFP that can overcome limited T cell persistence, particularly in the context of large tumor burdens (D'Aloia et al., 2018), we focused on Fas/Fas ligand (FasL) signaling, which normally delivers death signals to regulate immune responses (Peter et al., 2015). FasL expression has been detected in many tumors and TMEs (Yamamoto et al., 2019), including acute myeloid leukemia (Contini et al., 2007), ovarian (Motz et al., 2014), and pancreatic cancers (Kornmann et al., 2000); increased Fas signaling and subsequent CD8 T cell apoptosis were noted in acute myeloid leukemia patients (Contini et al., 2007). FasL is also up-regulated on activated T cells and can mediate activation-induced cell death (Villa-Morales and Fernández-Piqueras, 2012), which can substantially limit ACT efficacy.

[1]Program in Immunology, Fred Hutchinson Cancer Research Center, Seattle, WA; [2]Department of Medicine/Oncology, University of Washington, Seattle, WA.

Correspondence to Philip D. Greenberg: pgreen@u.washington.edu; Shannon K. Oda: shannon.oda@seattlechildrens.org.

We aimed to convert the Fas death signal to a costimulatory signal with the IFP platform. Comparisons of Fas IFPs with CD28 and 4-1BB costimulatory domains revealed that the trimeric Fas ectodomain (Villa-Morales and Fernández-Piqueras, 2012) could indeed enhance T cell function when paired with the 4-1BB intracellular domain, which requires trimerization to signal (Wyzgol et al., 2009). Our results demonstrate that a Fas-4-1BB IFP can overcome several obstacles to efficacy and improve ACT against liquid and solid tumors.

Results

Fas-4-1BB IFPs enhance proliferation and cytokine production of engineered T cells

We generated murine IFPs to combine the Fas ectodomain with the signaling endodomain of 4-1BB, with the transmembrane (tm) domain from either Fas (Fas_{tm}-4-1BB) or 4-1BB (Fas-4-$1BB_{tm}$; Fig. 1 A). Each IFP was linked to GFP by a P2A element, packaged in a retroviral vector (RV), and used to transduce murine P14 CD8 T cells, which express a TCR (TCR_{gp33}) specific for the gp33-41 epitope ($peptide_{gp33}$) of lymphocytic choriomeningitis virus (LCMV). Transduction increased Fas expression, which correlated with GFP signal strength (Fig. 1 B).

4-1BB signaling can enhance proliferation and function of T cells (Chen and Flies, 2013). To assess proliferation, engineered P14 T cells were stimulated with $peptide_{gp33}$-pulsed splenocytes. T cells expressing either Fas-4-1BB IFP construct (GFP^+) exhibited increased proliferation relative to T cells transduced with a GFP-only vector (Fig. 1, C and D). To investigate if IFP stimulation could induce proliferation in the absence of TCR signaling, we co-cultured T cells with an agonistic anti-Fas antibody (Jo2) or splenocytes without peptide. Proliferation was not observed in either condition (Fig. 1 D), supporting that Fas-4-1BB expression does not result in antigen-independent proliferation. To determine if the enhanced proliferation of IFP^+ cells resulted in a competitive advantage, a mixed population of IFP^+ and IFP^- T cells was repeatedly stimulated in vitro. After three stimulations, the proportion and viability of IFP-transduced P14 T cells was significantly increased (Figs. 1 E and S1 A; Figs. 1 F and S1 B).

As 4-1BB signaling in CD8 T cells can increase production of IL-2, which is a critical survival cytokine for T cells (Laderach et al., 2002), engineered T cells were stimulated in the presence of GolgiPlug (BD BioSciences) and assessed by flow cytometry. Both Fas-4-1BB IFPs significantly enhanced the proportion of IL-2–producing T cells (Fig. 1 G). We next questioned if the increased IL-2 production could potentially benefit IFP^- T cells. Proliferation was assessed in GFP-only control T cells cultured alone or co-cultured with Fas-4-1BB T cells at a 1:1 ratio. GFP-only control T cells exhibited enhanced proliferation in co-culture (Fig. 1 H), supporting a benefit provided by IFP cells in trans.

Studies with CAR T cells containing CD28 versus 4-1BB domains have revealed major phenotypic differences, including cell metabolism (Kawalekar et al., 2016), exhaustion, and in vivo persistence (Long et al., 2015). We engineered Fas-CD28 IFPs (Fig. S1 C) informed by our previous findings with CD200R-CD28 IFPs (Oda et al., 2017). The Fas_{tm}-$CD28_{cys}$ IFP exhibited low expression, but the Fas_{-9aas}-$CD28_{cys}$ IFP exhibited similar expression to the Fas-4-1BB IFPs (Fig. S1 D). Compared with the GFP-only control, and unlike the Fas-4-1BB and CD200R-CD28 IFPs, Fas-CD28 IFPs did not significantly enhance in vitro proliferation (Fig. S1, E and F), suggesting a dimerizing signaling domain is relatively ineffective when paired with the trimerizing Fas ectodomain.

4-1BB signaling can facilitate cytotoxic T cell function by inducing expression of the transcription factor eomesodermin (Eomes; Curran et al., 2013), and Fas-4-1BB–transduced P14 T cells expressed higher levels of intracellular Eomes, consistent with increased 4-1BB signaling (Fig. 1 I). When T cells were evaluated after in vitro restimulation, expression of either Fas-4-1BB IFP construct significantly increased polyfunctional effector cytokine production (Fig. 1 J). This was also antigen dependent, as the Fas agonist antibody alone did not induce cytokine production.

Fas-4-1BB improves in vitro function of tumor-responsive T cells

We selected the Fas-4-$1BB_{tm}$ IFP for further study (herein referred to as Fas-4-1BB). To assess T cell responses to endogenously presented antigen on tumor cells, we transduced CD8 TCR transgenic (TCR_{gag}) T cells specific for an epitope derived from Friend murine virus (F-MuLV)–induced leukemia (FBL; Oda et al., 2017; Öhlén et al., 2002; Teague et al., 2006), a murine leukemia cell line that expresses native FasL (Fig. 2 A). Transduced Fas-4-1BB TCR_{gag} T cells expressed Fas and GFP (Fig. 2 B) and were expanded with irradiated FBL cells and feeder splenocytes, modeling the rapid expansion protocol (REP) used with human T cells (Ho et al., 2006). We previously demonstrated enhanced CD28 costimulation with CD200R-CD28 IFPs that contain the native-sized ectodomain and colocalize to the immunological synapse (Oda et al., 2017). Native 4-1BB signaling also occurs in plasma membrane micropatches within the immunological synapse, where 4-1BB complexes are ligated by trimerized ligand (Sanchez-Paulete et al., 2016). When transduced TCR_{gag} T cells were co-cultured with FBL cells, FasL expression was detected on tumor cell surfaces but not on GFP-only control or Fas-4-1BB T cells (Fig. 2 C, blue). Low levels of endogenous Fas was expressed on GFP-only T cells, as measurable by flow cytometry (Fig. S2 A), but not detectable by microscopy. In contrast, Fas was readily evident on Fas-4-1BB–transduced T cells and concentrated at the T cell–tumor cell intersection (Fig. 2 C, red), demonstrating synapse localization.

We next assessed the impact of Fas-4-1BB expression on the proliferative response to endogenously presented tumor antigen by stimulating 100,000 transduced TCR_{gag} T cells with 6,250 FBL cells. Few GFP-only control T cells proliferated with this low-level stimulation; however, Fas-4-1BB T cells exhibited enhanced proliferation (Fig. 2, D and E), consistent with the finding that costimulation lowers the activation threshold (Nam et al., 2005; Nurieva et al., 2007; Sanchez-Paulete et al., 2016). The enhanced proliferation was observed despite coexpression of PD-L1 on FBL cells (Fig. S2 B). After three cycles of in vitro stimulation (Fig. S2 C), we measured increased fractions of IFP-

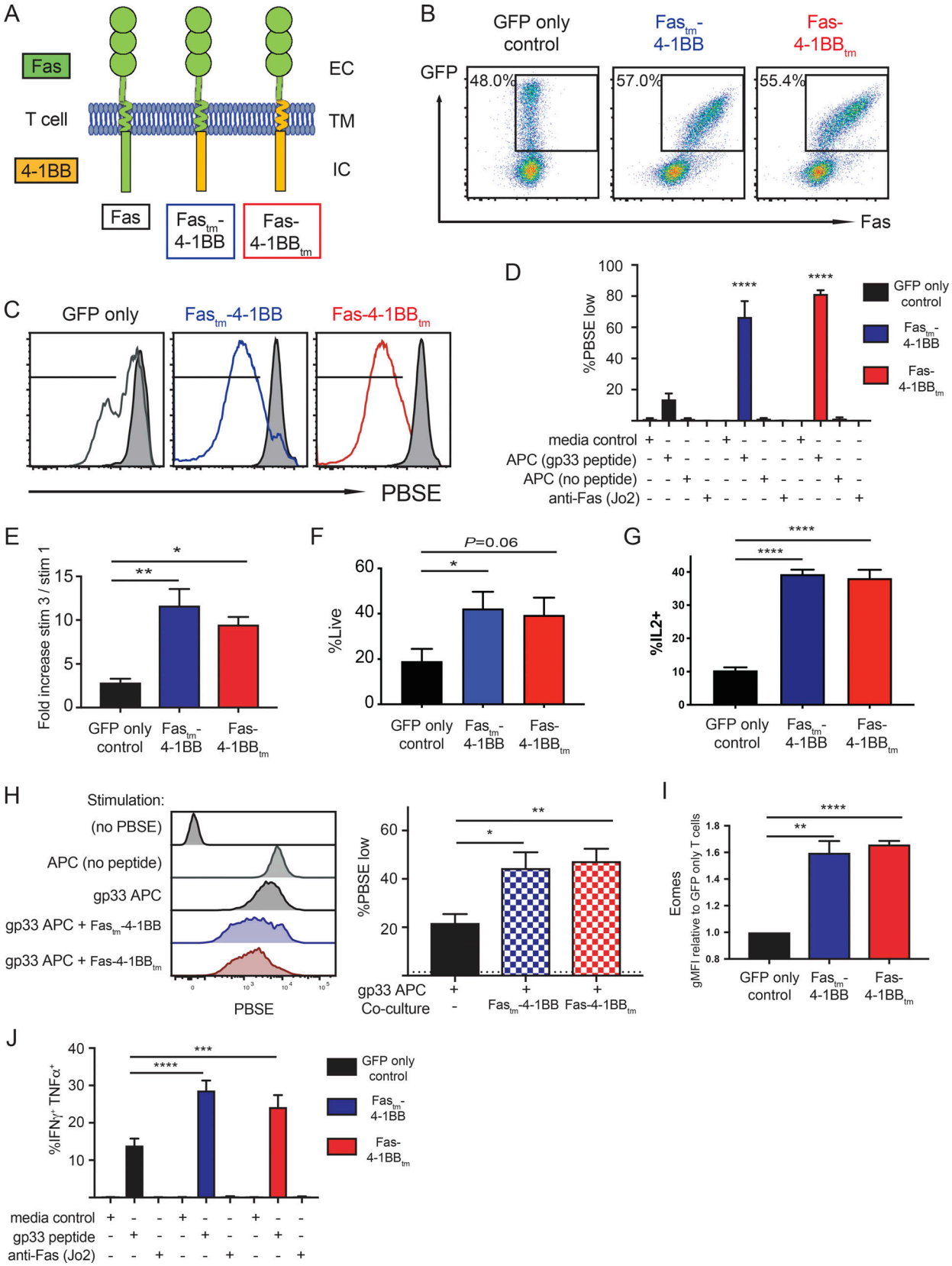

Figure 1. **Fas-4-1BB IFPs enhance proliferation and cytokine production of engineered T cells.** Splenocytes from naive P14 mice were stimulated with anti-CD3/CD28 antibodies and then transduced with retroviral supernatant. 7 d later, T cells were expanded by restimulation with peptide$_{Msln}$-pulsed irradiated splenocytes; this was repeated 7 d later. T cells were used for assays 5–7 d later. **(A)** Schematic representation of Fas-4-1BB IFP constructs. EC, extracellular; TM, transmembrane; IC, intracellular. **(B)** Expression of Fas on T cells transduced with GFP alone or Fas-4-1BB/GFP constructs, detected by flow

cytometry. **(C)** Proliferation of engineered GFP T cells 7 d after stimulation with peptide$_{gp33}$-pulsed splenocytes (1 µg/ml) relative to unstimulated T cells (gray). **(D)** Quantification of PBSE dilution in engineered GFP T cells 7 d after stimulation, as indicated. **(E)** Enrichment of transduced T cells in a mixed population of non- and transduced T cells. **(F)** Viability of GFP cells after three stimulations as determined by flow cytometry. **(G)** Proportion of T cells that exhibit intracellular IL-2 production after peptide$_{gp33}$ stimulation (1 µg/ml) for 5 h, assessed by flow cytometry. **(H)** Representative histogram and quantification of PBSE dilution in GFP-only control T cells 7 d after stimulation, as indicated, and co-culture with Fas$_{tm}$-4-1BB cells (blue) or Fas-4-1BB$_{tm}$ (red) P14 T cells. **(I)** Expression of Eomes in engineered T cells as detected by intracellular antibody staining and flow cytometry. gMFI, geometric MFI. **(J)** Effector cytokine production of engineered T cells after culture with media-only control, peptide$_{gp33}$ (1 µg/ml), or anti-Fas antibody (200 ng/ml) stimulation for 5 h, followed by intracellular cytokine flow cytometry. Data are representative of four (B) or three (C) experiments, or represent the mean of three (D, I, and J), four (E), seven (F), six (G), or two (H) experiments. *, P < 0.05; **, P < 0.01; ***, P < 0.001; ****, P < 0.0001 by one-way ANOVA for multiple comparisons (D, H, and J) or *t* test compared with GFP-only control T cells (E–G and I). Error bars indicate SEM.

expressing TCR$_{gag}$ T cells relative to GFP-only control T cells (Fig. 2 F), similar to the results using peptide stimulation (Fig. 1 E).

To determine if Fas-4-1BB expression impacted antitumor function, we assessed the ability of T cells to repeatedly lyse tumor cells in a serial-killing-over-time (SKO) assay that we developed using the IncuCyte instrument (Sartorius). T cells were combined with NucLight Red (Sartorius) FBL at a 3:1 ratio, and T cells were challenged with 10^4 FBL cells added every 24 h. GFP-only control and Fas-4-1BB T cells exhibited similar abilities to lyse the first round of tumor cells, quantified by the loss of red signal (Fig. 2 G). However, subsequent tumor cell additions revealed substantive differences; Fas-4-1BB T cells continued to efficiently lyse tumor cells, whereas control T cells killed fewer tumor cells with the second and third additions of FBL. To determine if Fas-4-1BB T cells exhibited superior per-cell function, T cells from the SKO assay were restimulated with FBL for 5 h. Expression of the Fas-4-1BB IFP construct significantly increased the proportion of cytokine-positive cells (IFNγ and TNFα; Fig. 2 H) and IFNγ production per cell (mean fluorescence intensity [MFI]; Fig. 2 I), supporting that Fas-4-1BB T cells sustained better function in the presence of persistent tumor targets.

We next investigated requirements for Fas-4-1BB function. The FBL cell line expresses the CD28 ligands CD80 and CD86 (Fig. S2 D), and we tested if a CD28 cosignal was necessary for Fas-4-1BB enhanced function. FBL were untreated or treated with blocking anti-CD80 and -CD86 antibodies and used to serially stimulate transduced T cells every 24 h, similar to the SKO assay that demonstrated enhanced tumor control with Fas-4-1BB T cells. We quantified FBL remaining 24 h after the last stimulation and found that CD28 ligand blockade did not impact the lysis of FBL tumor cells by Fas-4-1BB T cells (Fig. S2 E). FasL can be expressed on various cell types in the TME, including tumor and nontumor cells (e.g., endothelial cells, stromal cells, and myeloid cells; Zhu et al., 2019). To evaluate the contribution/requirement of tumor cell FasL expression, we treated FBL cells with a FasL-blocking antibody. Fas-4-1BB T cells exhibited a similar ability to lyse FasL-blocked FBL and untreated FBL in the SKO assay (Fig. 2 J). We also repeated proliferation (Fig. S2 F) and cytokine expression (Fig. S2 G) assays in the presence of tumor cell FasL blockade and observed that the activity of Fas-4-1BB T cells remained enhanced, suggesting that target cell FasL expression was not required for delivery of the signals through the IFP that enhance T cell function.

A decoy, truncated Fas receptor (trFas) that lacks the intracellular death domains has been shown to improve T cell function and ACT efficacy in murine models (Yamamoto et al., 2019). We found Fas surface expression to be higher in trFas T cells relative to Fas-4-1BB T cells (Fig. S2 H). Engineered trFas T cells exhibited enhanced proliferation and lytic function relative to GFP-only control T cells, but less than Fas-4-1BB T cells (Fig. S2, I and J). Thus, the decoy Fas activity and 4-1BB costimulatory signal apparently synergize to increase T cell function.

Fas-4-1BB signaling impacts T cell phenotype and improves ACT of murine leukemia

4-1BB signaling can promote cell cycle progression via TNF receptor–associated factor–dependent NF-κB activation, increased Bcl-2 expression, and PI3K and MEK-1/2 signaling pathway activations, including Akt phosphorylation (Chen and Flies, 2013; Kroon et al., 2007; Lee et al., 2013). Following stimulation, Fas-4-1BB T cells exhibited increased expression of Bcl-2 and pAkt relative to GFP-only control T cells (Fig. 3, A and B). Unstimulated Fas-4-1BB and GFP-only T cells exhibited similar pAkt expression, supporting a lack of IFP tonic signaling (Fig. S3 A). Robust T cell activation can result in generally increased protein expression (Seedhom et al., 2016), but pro-apoptotic Bcl-2–associated X (Bax) protein expression was not preferentially increased in Fas-4-1BB T cells (Fig. S3 B), suggesting that Bcl-2 and pAkt expression was specifically induced by Fas-4-1BB signaling.

4-1BB signaling also impacts T cell metabolism, enhancing mitochondrial biogenesis and fatty acid metabolism, and in vivo 4-1BB signaling can improve ACT of solid tumors in mouse models (Choi et al., 2017; Kawalekar et al., 2016; Menk et al., 2018). In particular, spare respiratory capacity indicates the capacity of cells to produce energy in response to increased stress, which is associated with increased cell survival and CD8 T cell memory development (van der Windt et al., 2012). We examined the metabolic profiles of transduced T cells after three in vitro stimulations to allow sufficient time for Fas-4-1BB signaling to potentially impact the T cell metabolic program. We found that GFP-only control and Fas-4-1BB T cells exhibited similar basal oxygen consumption rates (OCRs; Fig. 3 C), but Fas-4-1BB T cells displayed higher spare respiratory capacity than GFP-only control T cells (Fig. 3, C and D), as previously shown for 4-1BB–stimulated T cells (Kawalekar et al., 2016; Menk et al., 2018). Fas-4-1BB–expressing T cells exhibited increased mitochondrial density by confocal microscopy, consistent with mitochondrial biogenesis (Fig. 3 E). These data together suggest that Fas-4-1BB expression induces 4-1BB signaling, including altered metabolism with increased mitochondrial density.

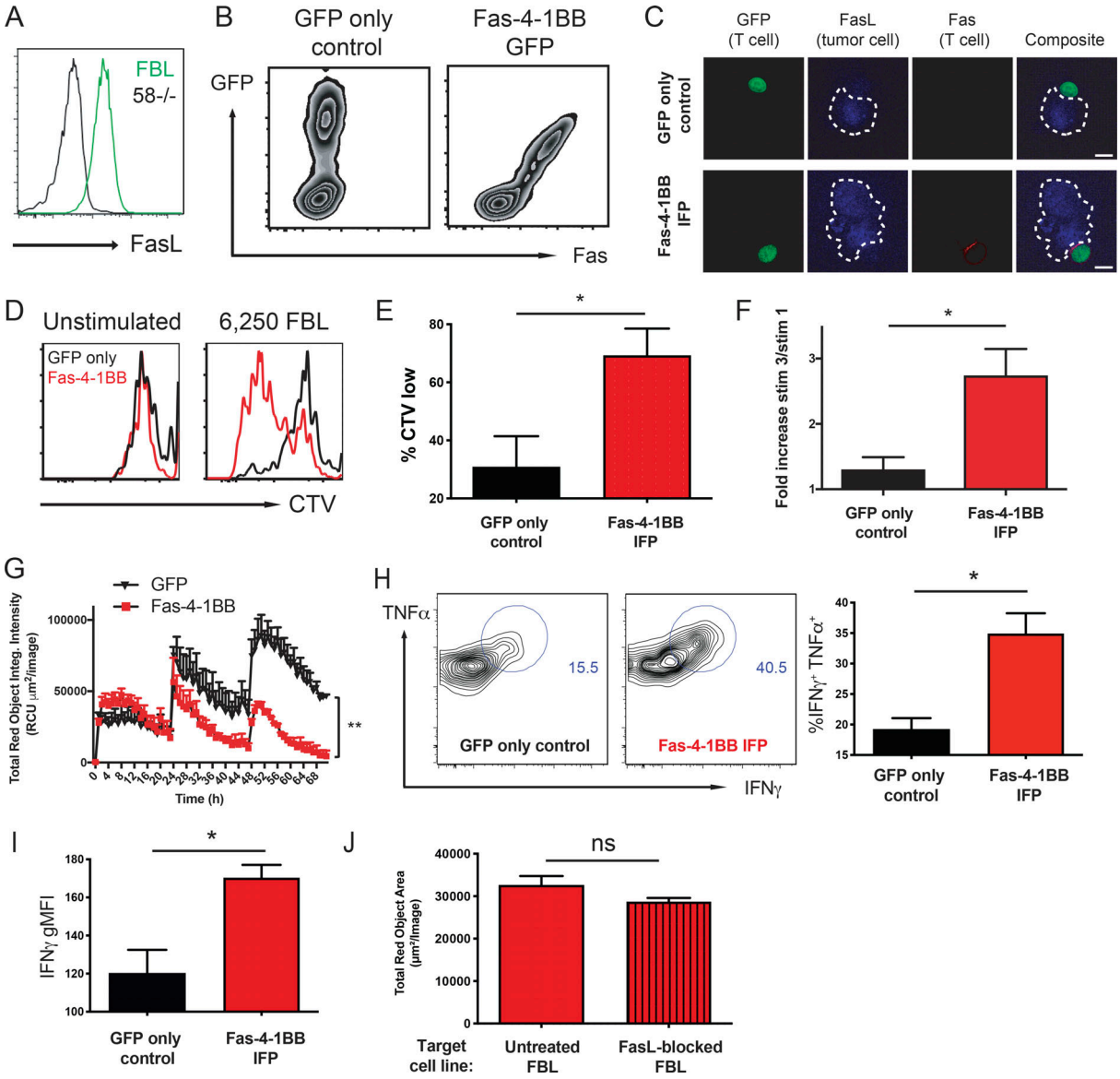

Figure 2. **Fas-4-1BB expression enhances function of transduced T cells.** Splenocytes from naive TCR_{gag} mice were transduced, restimulated once with irradiated FBL and splenocytes, and assayed 5–7 d later. **(A)** Expression of FasL in FBL and $58^{-/-}$ murine cell lines as detected by flow cytometry. **(B)** Transgenic expression of Fas on engineered T cells as detected by flow cytometry for GFP and anti-Fas antibodies. **(C)** Visualization of Fas-4-1BB localization within T cell–FBL conjugates. Engineered T cells were co-cultured with FBL at a 10:1 ratio, and conjugates were imaged by confocal microscopy. Scale bars indicate 10 µm. **(D)** Proliferation of Fas-4-1BB (red) and GFP empty vector control (black) T cells (100,000 cells) as measured by cell trace violet (CTV) dilution without or after stimulation with 6,250 FBL for 7 d. **(E)** Quantification of CTV dilution of Fas-4-1BB T cells (representative in D) relative to CTV dilution of GFP empty vector control T cells. **(F)** Enrichment of transduced T cells in a mixed population that also included nontransduced TCR_{gag} T cells after two weekly cycles of restimulation with irradiated FBL and splenocytes. **(G)** IncuCyte SKO assay. NucLight Red⁺ FBL were co-cultured with GFP control (black) or Fas-4-1BB (red) T cells at a 3:1 ratio (10^4 FBL). 10^4 FBL were added every 24 h, and tumor cell lysis was quantified by Total Red Object Integrated Intensity (red calibrated unit [RCU] µm²/image). **(H)** Cytokine production of T cells after SKO assay. T cells were restimulated with FBL (1:1) for 5 h, fixed, permeabilized, stained for intracellular cytokines, and assessed by flow cytometry. **(I)** Geometric MFI (gMFI) of IFNγ production in H. **(J)** NucLight Red⁺ FBL were untreated or treated with blocking anti-FasL antibody and used to stimulate Fas-4-1BB transduced T cells every 24 h for three stimulations. 24 h following the last stimulation, the remaining FBL were quantified by IncuCyte analysis. Data are representative of two (A, C, and G), five (B), or six (D) experiments or represent the mean of six (E) or three (F and H–J) experiments. ns, not significant; *, $P < 0.05$ by *t* test (E, F, and H–J) and at the final time point (G). Error bars indicate SEM.

As Fas-4-1BB expression significantly improved in vitro T cell function, we next tested whether this engineering strategy would be sufficient to improve anti-leukemia ACT efficacy. Mice were injected with a lethal dose (4×10^6 i.p.) of FBL cells, which were allowed to disseminate for 5 d. Following a single round of cyclophosphamide (Cy; 180 mg/kg) and engineered T cell therapy, mice were monitored for 100 d and euthanized upon signs of morbidity. We had shown that therapy with the $CD200R_{-9aas}$-$CD28_{cys}$ IFP can improve mouse survival (Oda et al., 2017), but the Fas-CD28 IFP did not enhance survival in the FBL model (Fig. S3 C), consistent with the disappointing in vitro results with this construct.

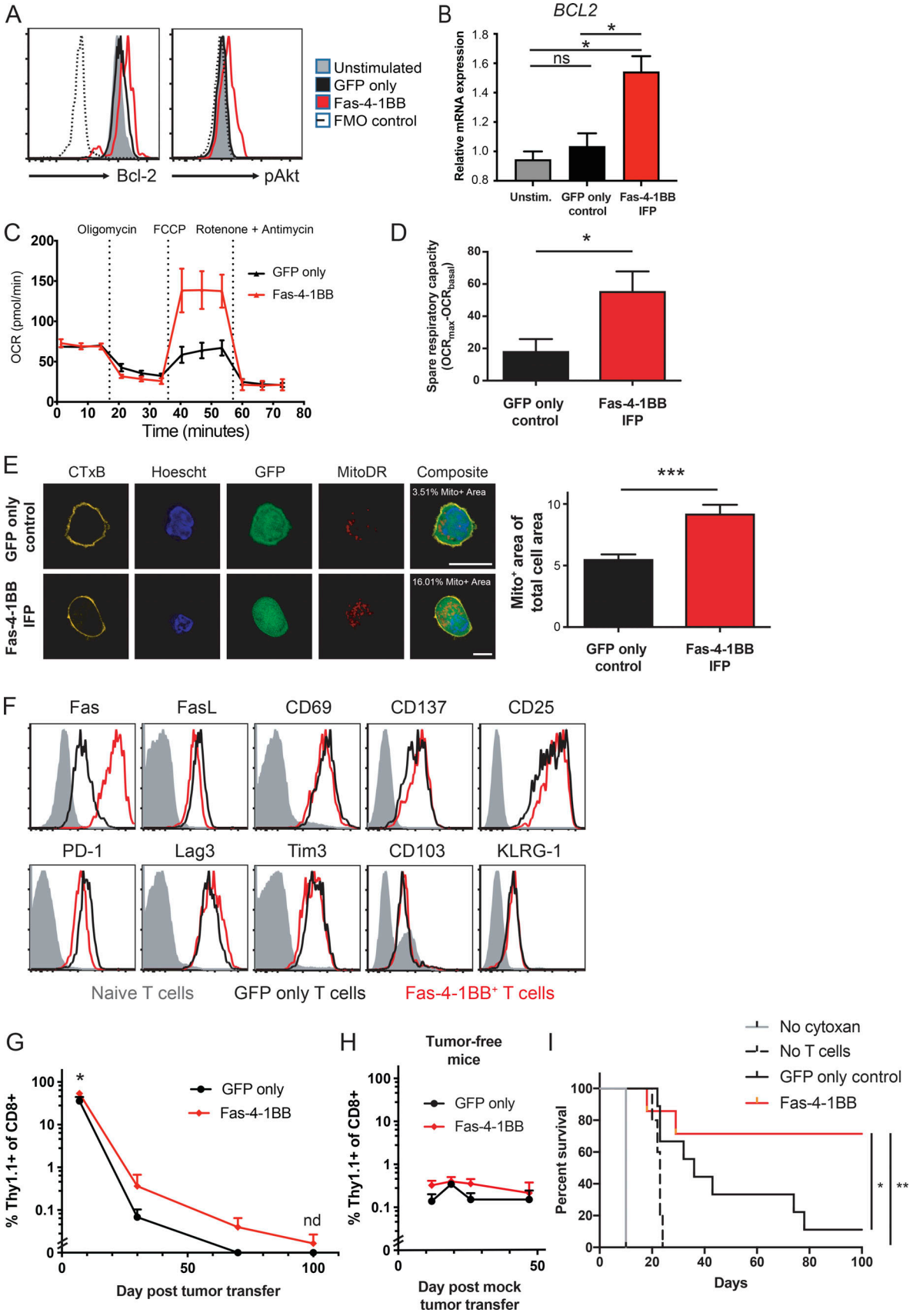

Figure 3. **Fas-4-1BB expression alters the phenotype of transduced T cells and improves ACT efficacy in a murine leukemia model**. Transduced TCR_{gag} T cells were generated as described in Fig. 2. **(A)** Expression of anti-apoptotic and cell growth/survival factors in engineered T cells. Transduced T cells were

incubated overnight with FBL tumor cells at a 1:1 ratio and then were fixed, permeabilized, and stained for intracellular pAKT and Bcl-2. FMO, fluorescence minus one. **(B)** Quantitative PCR of *BCL2*. GFP control and Fas-4-1BB T cells were FACS isolated and relative expression determined with the qPCR SYBR Green Assay and analyzed by the ΔΔCT method. **(C)** Metabolic profile of engineered T cells. Twice-restimulated T cells were assessed for OCR under basal metabolic conditions and in response to mitochondrial inhibitors. A representative OCR trace of GFP-only control (black) or Fas-4-1BB (red) T cells is shown. **(D)** Cumulative spare respiratory capacity of T cells as in panel C. **(E)** Quantification of the percentage of cell area occupied by mitochondria. Confocal images of engineered GFP$^+$ (green) T cells stained with CTxB (yellow), Hoechst (blue), and MitoDR (red; n = 19–20 independent images per group). Scale bars indicate 10 µm. **(F)** Phenotype of transduced, twice-stimulated T cells on day of injection. **(G–I)** B6 mice were injected with 4 × 10^6 FBL cells or mock injected (I). 5 d later, mice were treated with Cy and a cohort received 10^6 GFP-only control or Fas-4-1BB T cells i.p. **(G)** Persistence of tumor-specific T cells in surviving FBL-bearing mice that received GFP-only control (n = 9) or Fas-4-1BB (n = 7) T cells. Mice were bled at days 12, 30, 70, and 100 after tumor transfer and transferred T cells detected by congenic marker expression as assessed by flow cytometry. **(H)** Persistence of tumor-specific T cells in tumor-free mice. Mice were bled at days 12, 19, 26, and 47 after tumor transfer. Transferred T cells were detected by congenic marker expression as assessed by flow cytometry (n = 4/group). **(I)** Survival of FBL-bearing mice that received no treatment (n = 1), Cy only (n = 10), or Cy plus GFP control (n = 9) or Fas-4-1BB (n = 7) T cells. Data are representative of two (A), three (F), four (C), or one (H) experiment or represent the mean of three (B), two (E, G, and I), or four (D) experiments. ns, not significant; *, $P < 0.05$; **, $P < 0.01$; ***, $P < 0.001$ by t test (B and D) and at each time point (G and H), or by log-rank Mantel-Cox test (I). Statistics not done if n < 3/group. Error bars indicate SEM.

Although we observed functional superiority of Fas-4-1BB IFP T cells in vitro, surface marker expression was similar to GFP-only control T cells on the day of injection (Fig. 3 F). Elevated levels of Fas-4-1BB T cells were detected in the blood but did not show uncontrolled proliferation (Fig. 3 G). When T cells were transferred to tumor-free mice that received the same Cy-preconditioning regimen (Fig. 3 H), Fas-4-1BB expression did not produce in vivo T cell expansion in the absence of specific TCR antigen, as observed with our in vitro study (Fig. 1 D). All mice that were untreated or received only Cy succumbed to disease by day 10 or 25, respectively (Fig. 3 I), consistent with our previous results (Oda et al., 2017; Stromnes et al., 2010). ACT with GFP-only tumor-specific T cells modestly increased survival to 11%, while ACT with Fas-4-1BB T cells improved survival to 71%. A survival study with trFas T cells again revealed an intermediate effect, improving survival relative to untreated and Cy-treated mice but reducing persistence and ACT therapeutic efficacy relative to Fas-4-1BB T cells (Fig. S3, D and E). Thus, adding Fas-4-1BB IFP engineering to T cells resulted in significantly enhanced therapeutic efficacy in the leukemia model.

Fas-4-1BB improves ACT in an autochthonous tumor model of pancreatic cancer

Solid tumors commonly exhibit an inhibitory TME that blocks T cell accumulation (Anderson et al., 2017; D'Aloia et al., 2018). We previously developed a murine TCR targeting the mesothelin (Msln) antigen; TCR_{Msln} T cells mediated antitumor efficacy but progressively up-regulated exhaustion markers and lost function in pancreatic (Stromnes et al., 2015) and ovarian (Anderson et al., 2019) tumor models. To determine if the Fas-4-1BB IFP could improve T cell persistence and antitumor activity, we generated a three-gene retroviral construct with the IFP and the β and α chains of TCR_{Msln} (Stromnes et al., 2015). TCR_{Msln} and TCR_{Msln}/Fas-4-1BB T cells expressed high TCR levels, and IFP-transduced T cells exhibited increased Fas expression (Fig. 4, A and B); >95% of T cells expressed the transduced proteins after restimulation with Msln peptide (Fig. 4 A). After two in vitro stimulations, both sets of engineered T cells exhibited similarly increased expression of activation/exhaustion markers relative to untransduced T cells (Fig. 4 C).

Upon FasL engagement, Fas recruits Fas-associated death domain protein and pro–caspase-8, which is cleaved to its active form and then activates downstream caspases to mediate cell death (Li et al., 1998). To evaluate a potential decoy mechanism for the Fas-4-1BB IFP, we used caspase-8 activation as a surrogate readout of endogenous Fas signaling. Fas-deficient T cells (from Fas^{lpr} mice) as expected expressed the lowest levels of activated caspase-8, followed by TCR_{Msln}/Fas-4-1BB T cells and then TCR_{Msln} T cells (Fig. 4 D). The difference between TCR_{Msln}/Fas-4-1BB T cells and TCR_{Msln} T cells did not reach statistical significance, which might reflect the death and elimination of TCR_{Msln} T cells with intact Fas signaling.

The genetically engineered $Kras^{LSL\text{-}G12D/+}Trp53^{LSL\text{-}R172H/+}p48^{Cre/+}$ (KPC) mouse model of pancreatic cancer features autochthonous tumors with elevated Msln and FasL expression (Mills et al., 2014; Stromnes et al., 2015). KPC mice spontaneously and continuously generate pancreatic tumors, and the TME recapitulates the immunosuppressive TME characteristics of human disease (Lee et al., 2016). Having previously characterized TCR_{Msln}-T ACT in KPC mice (Stromnes et al., 2015), we asked if Fas-4-1BB expression could enhance ACT efficacy. We enrolled KPC mice to study when 3-mm tumors were detected by ultrasound. Equal numbers of TCR_{Msln} and TCR_{Msln}/Fas-4-1BB IFP T cells were combined and injected into Cy-conditioned KPC mice; 7 and 28 d later, cohorts of mice were euthanized and tumor-infiltrating lymphocytes (TILs) analyzed. TCR_{Msln}/Fas-4-1BB T cells were more highly represented in tumors at both time points (Fig. 4 E) and exhibited modestly increased cytokine production at day 7 (Fig. S4 A). We measured similar levels of PD-1 expression on both T cell populations but slightly reduced Tim3 and Lag3 expression on TCR_{Msln}/Fas-4-1BB T cells, suggesting potentially reduced/delayed expression of receptors associated with functional exhaustion (Fig. 4 F). We also analyzed organs that express endogenous Msln (Bera and Pastan, 2000; Hassan et al., 2004). Relative to control mice that did not receive T cells, immunohistochemical analyses revealed no CD3$^+$ T cell accumulation in hearts or lungs of KPC mice 28 d after transfer of TCR_{Msln}/Fas-4-1BB T cells (Fig. S4 B), as we previously reported for transferred TCR_{Msln} T cells (Stromnes et al., 2015).

To determine if Fas-4-1BB–engineered T cells can enhance ACT efficacy, we conducted a rolling enrollment survival study. KPC mice were screened and enrolled as described above, with no significant enrollment age difference between the randomized ACT treatment groups (Fig. 4 G). We had previously shown

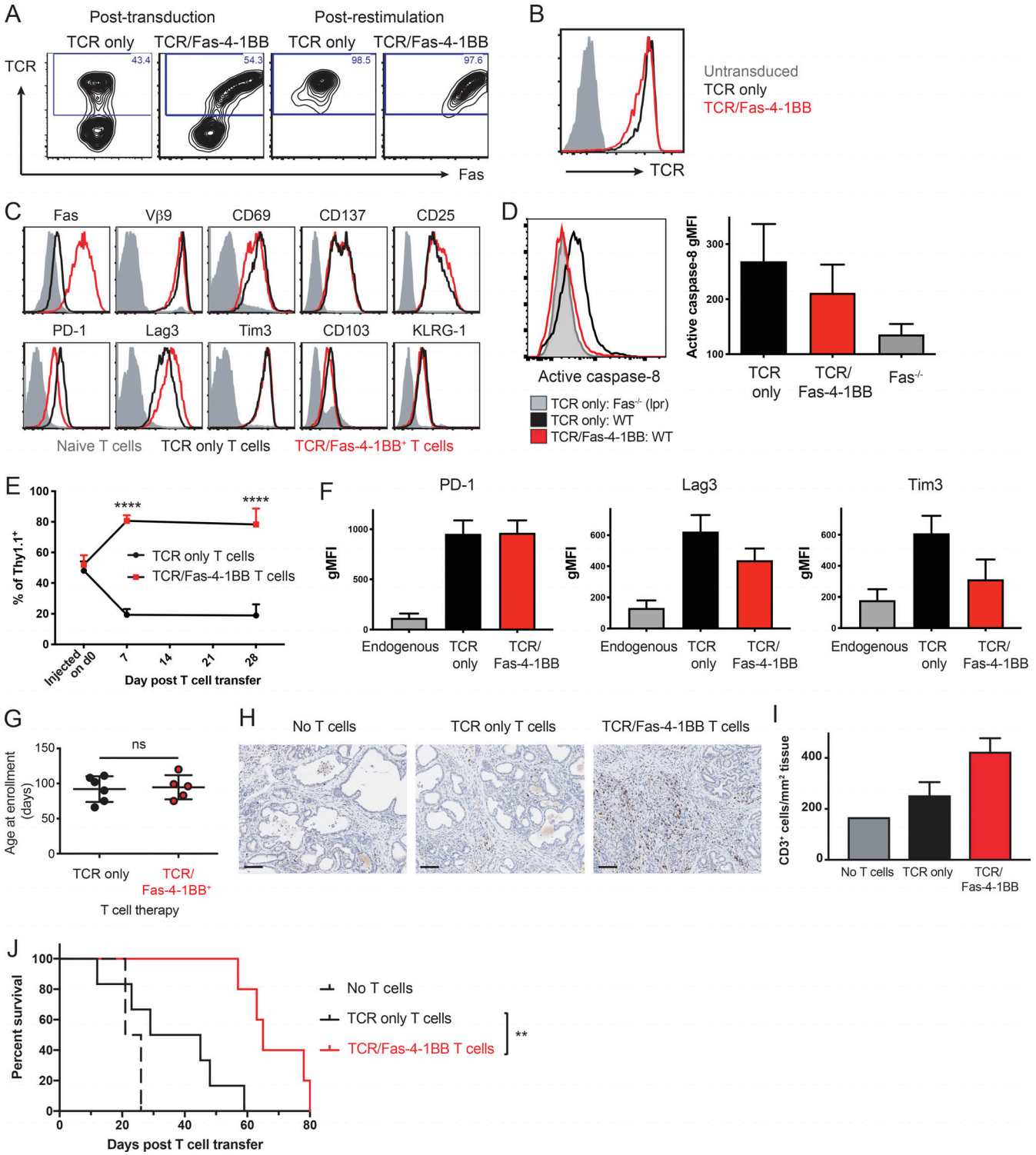

Figure 4. **Fas-4-1BB T cells preferentially accumulate in the tumor and significantly improve survival in the KPC pancreatic cancer model.** Splenocytes from P14 mice were transduced and restimulated/expanded with irradiated peptide$_{Msln}$-pulsed splenocytes. T cells were assayed 5–7 d after the last stimulation. **(A)** T cell expression of Fas and TCR$_{Msln}$, as detected by Vβ9 staining and flow cytometry. **(B)** Expression of TCR$_{Msln}$ as detected by Vβ9 expression in transduced T cells after restimulation relative to untransduced T cells (gray). **(C)** The expression of surface molecules on TCR$_{Msln}$ (black) and TCR$_{Msln}$/Fas-4-1BB (red) T cells 5 d after restimulation compared with unstimulated T cells (gray). **(D)** Expression of activated caspase-8 in engineered T cells. T cells were stained 7 d after restimulation with the Vybrant FAM Caspase-8 Assay Kit (ThermoFisher) and analyzed by flow cytometry (differences with IFP did not reach statistical significance). gMFI, geometric MFI. **(E–J)** Weekly high-resolution ultrasound screening of KPC mice was initiated at 8 wk of age, and mice were enrolled in the study following detection of a pancreatic tumor with a minimum diameter of 3 mm. Mice were treated with a combination therapy of Cy (before first infusion only), T cell infusion, and tumor antigen vaccination (peptide$_{Msln}$-pulsed irradiated splenocytes). **(E)** Preferential accumulation of Fas-4-1BB T cells in tumor tissue. Congenically distinct TCR$_{Msln}$ (black) and TCR$_{Msln}$/Fas-4-1BB (red) T cells (Thy1.1$^{+/+}$ and Thy1.1$^{+/-}$, respectively) were combined at a 1:1 ratio

(5 × 10^6 each) and transferred to KPC mice. 7 d and 28 d after a single infusion, pancreas TIL were assessed by flow cytometry (day 7, *n* = 3; day 28, *n* = 4). **(F)** Phenotype of transferred T cells at day 28 in E relative to endogenous T cells in tumor (*n* = 4/group; TCR/Fas-4-1BB versus TCR only, P = not significant for all markers). **(G)** Age of enrollment in a survival study. Mice were randomly assigned to treatment groups of TCR_{Msln} (black, *n* = 6) or TCR_{Msln}/Fas-4-1BB (red, *n* = 5) T cell therapy. **(H)** IHC for $CD3^+$ cells in pancreas from mice that received the indicated therapy every 2 wk for a total of three infusions, with Cy administered before the first infusion only. Mice were euthanized following signs of morbidity. Scale bars indicate 100 µm. **(I)** As in H, quantification of $CD3^+$ cells in tumor tissue from mice that received no T cells (*n* = 1), TCR_{Msln}-only T cells (*n* = 2), or TCR_{Msln}/Fas-4-1BB T cells (*n* = 3). **(J)** Survival of KPC mice that received Cy and $peptide_{Msln}$-pulsed splenocytes and either no ACT (dashed, *n* = 2), TCR_{Msln} (black, *n* = 6), or TCR_{Msln}/Fas-4-1BB (red, *n* = 5) ACT. Mice received infusions every 2 wk for a total of three infusions, with Cy administered before the first infusion only. Data are representative of three (A and B) or two (C and H) experiments or represent the mean of two to five (D–G, I, and J) experiments. ns, not significant; **, P < 0.01; ****, P < 0.0001 by *t* test (D, F, and G) and at each time point (E), or by log-rank Mantel-Cox test (J). Error bars indicate SEM.

efficacy with a combination therapy of Cy (before first infusion only), T cell infusion, tumor antigen vaccination ($peptide_{Msln}$-pulsed irradiated splenocytes), and IL-2 therapy; this regimen was repeated every 2 wk for the study duration to provide an ongoing source of functional T cells (Stromnes et al., 2015). To create a more challenging scenario for T cell therapy and to avoid IL-2 therapy that can result in toxicity and promotion of inhibitory T regulatory cells (Jiang et al., 2016), we altered therapy to omit IL-2 injections and reduce T cell infusions to a total of three. Mice were euthanized for disease progression (lethargy and hind-limb paralysis), and tumor samples were analyzed by immunohistochemistry (IHC); increased $CD3^+$ TILs were detected in samples from mice treated with TCR_{Msln}/Fas-4-1BB T cells relative to samples from mice who received TCR_{Msln} T cells or no ACT (Fig. 4, H and I). Consistent with our previous findings, TCR_{Msln} T cell therapy enhanced survival relative to Cy treatment alone (Fig. 4 J). Treatment with TCR_{Msln}/Fas-4-1BB T cells significantly further enhanced survival, resulting in a median survival of 65 d versus 37 d with TCR_{Msln} T cells. All TCR_{Msln}/Fas-4-1BB T cell recipients (four out of four) exhibited T cell persistence, whereas the sole survivor that received TCR_{Msln} T cells had no detectable persistence in the blood 28 d after the final infusion (Fig. S4 C).

A human Fas-4-1BB IFP enhances primary human T cell function

To examine Fas-4-1BB in a human cancer setting, we used the Panc1 human pancreatic cell line. As FasL can be cleaved from the surface of cells by matrix metalloproteinase (MMP) activity (Poulaki et al., 2001), we treated Panc1 cells with an MMP inhibitor overnight (Batimastat, Abcam). Panc1 cells exhibited a low level of FasL expression that was increased with MMP inhibitor treatment (Fig. 5 A).

As with the murine IFPs, we generated two Fas-4-1BB constructs with different transmembrane domains (Fig. 1 A), as well as a trFas control construct that lacks the intracellular signaling domain, to serve as a decoy receptor. The constructs were inserted into single lentiviral vectors with the β and α chains of the HLA-A2–restricted $MSLN_{530-538}$-specific TCR (TCR_{MSLN}) that we previously isolated from a healthy human donor (Stromnes et al., 2015). Human primary T cells transduced to express TCR_{MSLN} and a Fas construct exhibited equivalent levels of TCR_{MSLN} expression as T cells transduced with TCR_{MSLN} alone (Fig. 5 B). In contrast with the murine studies, Fas expression varied from higher to lower intensity staining: trFas, Fas-4-$1BB_{tm}$, and Fas_{tm}-4-1BB. We selected Fas_{tm}-4-1BB for additional study.

T cells were transduced and then twice restimulated with irradiated feeder cells and anti-CD3 antibodies (REP; Ho et al., 2006). In an expansion stress test, T cells were cultured in the absence of supportive cytokines, including IL-2. TCR_{MSLN}/Fas_{tm}-4-1BB T cells exhibited the greatest expansion, followed by the decoy TCR_{MSLN}/trFas and then TCR_{MSLN}-only T cells, suggesting that both FasL-binding and 4-1BB signaling activities contribute to increased accumulation in vitro (Fig. 5 C). To determine if TCR_{MSLN}/Fas_{tm}-4-1BB T cells retained more efficient effector function after multiple stimulations, we co-cultured twice-stimulated T cells with T2 cells pulsed with $peptide_{MSLN}$ and then assessed IFNγ production by ELISA. TCR_{MSLN}/trFas and TCR_{MSLN}-only T cells exhibited similar cytokine production, whereas TCR_{MSLN}/Fas_{tm}-4-1BB T cells produced higher levels of IFNγ (Fig. 5 D).

We next tested whether TCR_{MSLN}/Fas_{tm}-4-1BB T cells could enhance lysis of human tumor cells. NucLight Red (Sartorius) Panc1 cells were allowed to adhere to plates overnight, T cells were added, and tumor cell lysis was quantified by IncuCyte analysis. TCR_{MSLN} and TCR_{MSLN}/trFas T cells controlled tumor growth similarly, revealing that expression of a decoy Fas receptor alone was not sufficient to enhance/sustain T cell lytic ability (Figs. 5 E and S5 A). In contrast, TCR_{MSLN}/Fas_{tm}-4-1BB T cells lysed significantly more tumor cells than did TCR_{MSLN}-only T cells. T cells previously exposed to a tumor in the IncuCyte assay were then cultured with fresh Panc1 cells and stained for Lamp-1 (CD107a), a marker of activation and cytotoxic degranulation (Aktas et al., 2009). TCR_{MSLN}/trFas T cells exhibited less Lamp-1 expression than TCR_{MSLN}-only T cells, whereas TCR_{MSLN}/Fas_{tm}-4-1BB trended to increased expression (Fig. S5 B). We conclude that Fas-4-1BB expression modestly increases effector cytokine production and significantly enhances T cell expansion, which together lead to enhanced lysis of tumor targets.

Discussion

Adoptive T cell immunotherapy has produced impressive results against hematologic malignancies but insufficient efficacy against solid tumors to date. We have now developed an engineering approach to enhance the in vivo persistence and antitumor efficacy of transferred T cells. Our targeted, two-hit strategy uses a single fusion protein to both overcome a death signal prevalent in the TME of many cancers (Contini et al., 2007; Kornmann et al., 2000; Motz et al., 2014; Peter et al., 2015; Yamamoto et al., 2019) and on activated T cells (Villa-Morales

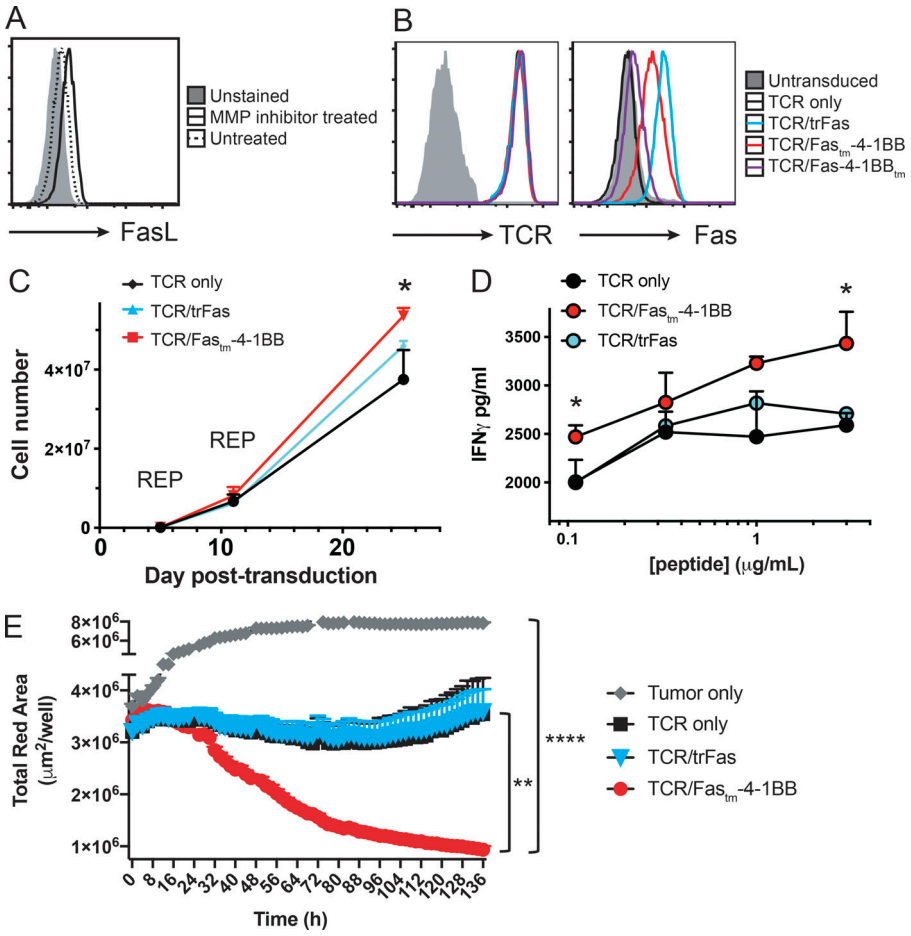

Figure 5. **A Fas-4-1BB IFP enhances primary human T cell function. (A)** FasL expression in human Panc1 cell line. Panc1 cells were incubated with MMP inhibitor overnight (solid) or left untreated (dotted) and analyzed for FasL expression by flow cytometry, compared with unstained Panc1 cells (gray). Representative of two independent studies. **(B–E)** CD8 T cells from healthy HLA-A2$^+$ donor PBMCs were stimulated with anti-CD3/CD28 Dynabeads and transduced with lentiviral supernatant. Transduced T cells were isolated by FACS and restimulated by REP every 10–14 d in the presence of IL-2. Data are shown as mean ± SEM. **(B)** Expression of TCR_{MSLN} and Fas in primary human T cells as detected by $MSLN_{530}$/HLA-A2 tetramer and anti-Fas antibody staining and flow cytometry. Representative of two independent studies. **(C)** T cell expansion with multiple REP stimulations in the absence of cytokines. T cells were restimulated by REP on days 5 and 11 and again counted on day 26 after transduction. Data represent the mean of experiments using T cells from three unique human donors. *, P < 0.05, two-way ANOVA. **(D)** IFNγ production as quantified by ELISA. Transduced T cells were twice REP restimulated. 7 d following the last REP, T cells were cultured with T2 cells pulsed with a titration of $peptide_{MSLN}$ for an additional 7 d. IFNγ production in the supernatant was quantified by ELISA. Assay performed in triplicate. *, P < 0.05, *t* test. **(E)** Lysis of pancreatic tumor cells as detected by IncuCyte analysis. NucLight Red$^+$ Panc1 cells were cultured alone (gray) or co-cultured with TCR-only (black), TCR/trFas (blue), or TCR/Fas-4-1BB (red) T cells at a 30:1 E:T ratio in triplicate. Tumor cell concentration was determined by Total Red Area (μm^2/well). Representative of three independent experiments. Statistical analyses are shown: TCR/Fas_{tm}-4-1BB versus TCR only, **, P = 0.004; TCR/Fas_{tm}-4-1BB versus tumor only, ****, P < 0.0001; *t* test of final time point.

and Fernández-Piqueras, 2012) and provides a pro-survival costimulatory signal to T cells. Our results suggest that this fusion protein can increase T cell function when combined with murine or human TCRs and can significantly improve therapeutic efficacy in in vivo models of liquid and solid tumors.

Checkpoint blockade and activation of costimulatory molecules have shown antitumor efficacy, but these therapies engage receptors on cell types other than the tumor-reactive T cells, with systemic toxicity risks, especially in combination therapies (Ribas and Wolchok, 2018). In particular, 4-1BB agonist therapy has produced severe hepatitis in clinical trials (Bartkowiak and Curran, 2015). Another approach is to express 4-1BB ligand on engineered T cells, which can provide an auto-costimulatory signal (Stephan et al., 2007), but also potentially to endogenous T cells, increasing the risk of autoimmunity or other unwanted responses. In contrast, the IFP platform allows exclusive delivery of costimulatory signals to the genetically engineered, tumor-targeting T cells and provides a decoy for a death receptor via the Fas ectodomain. We hypothesized that optimal activity might require the intentional pairing of IFP costimulatory endodomains with ectodomains that match the native signaling requirements of the costimulatory domain (e.g., dimer or trimer). We have now shown that we can combine domains from two trimeric receptors (Fas and 4-1BB) to produce effective costimulation—the Fas-4-1BB IFP enhanced the therapeutic potential of TCR-T cells in murine models of leukemia and pancreatic cancer and improved in vitro function of human primary T cells. Interestingly, several assays showed increasingly improved function of Fas-4-1BB T cells after multiple stimulations (Fig. 1, F and G; Fig. S1, A and B; Fig. 2, F and G; and Fig. S2 C), suggesting a combination of diminished activity of control T cells and an enhanced cellular product with Fas-4-1BB expression. A recent study using a pooled knock-in screen to evaluate synthetic engineering strategies for enhancement of T cell function affirmed that FasL targeting can significantly promote proliferation and survival in vitro, but in vivo studies were not pursued (Roth et al., 2020). We are now pairing other

trimeric costimulatory signaling domains with the Fas ectodomain and evaluating T cell programming differences subsequent to signaling to identify and advance optimally effective IFPs.

A potential concern is that interference with endogenous Fas signaling could cause lymphoproliferative disease or lymphomagenesis; however, we did not observe expansion of Fas-4-1BB T cells upon transfer to tumor-free mice that lack the TCR-recognized tumor antigen (relative to TCR-only T cells; Fig. 3 H). Thus, expression of Fas-4-1BB IFP alone did not induce proliferation in response to endogenous FasL. These data contrast with studies performed with T cells isolated from Fas-deficient *lpr* mice, which do feature hyperproliferation and autoimmune disease (Watanabe-Fukunaga et al., 1992). However, *lpr* T cells develop in the thymus without Fas signaling, whereas Fas-4-1BB T cells develop with Fas signaling and have a low level of endogenous Fas signaling. We did not observe lymphomagenesis in our long-term (>100 d) in vivo studies, but an inducible suicide-gene system could be clinically used to protect against such a possibility.

Diverse FasL sources can induce T cell–associated Fas signaling and resultant apoptosis. Abnormally high FasL transcript levels were recently reported for a majority of tumors (Yamamoto et al., 2019), and higher FasL protein expression is commonly associated with worsened prognosis (Peter et al., 2015). In fact, TME expression of FasL may often be underestimated, as many fixation methods limit binding of specific anti-FasL antibodies (Vekemans et al., 2004) and FasL can be released in tumor exosomes that can mediate T cell apoptosis even when cell surface FasL is undetected (Klinker et al., 2014). FasL can also inhibit antitumor T cell activity when expressed by nontumor TME cells, as with the tumor vascular endothelium of ovarian, colon, and other solid tumors that can restrict T cell infiltration (Ichinose et al., 2001; Motz et al., 2014). T cells also up-regulate FasL in response to stimulation, enabling T cells to exert effector function by eliminating Fas^+ cells, but FasL up-regulation can reduce the effector T cell population after an immune response (Thome and Tschopp, 2001). The transition of T cells from a Fas-insensitive effector phase to a Fas-sensitive deletion phase is controlled by expression of the FLICE inhibitory protein (FLIP; Thome and Tschopp, 2001; Villa-Morales and Fernández-Piqueras, 2012), which binds and inhibits caspase-8 activation and subsequent apoptosis (Thome and Tschopp, 2001). Reduced FLIP expression is associated with chronic stimulation and tonic signaling in 4-1BB CAR T cells, increasing activation-induced cell death and limiting ACT efficacy (Gomes-Silva et al., 2017; Künkele et al., 2015). Here, we show that Fas-4-1BB–expressing T cells exhibit reduced caspase-8 activation, suggesting that the IFP can substitute for protective FLIP expression. Thus, IFP expression can potentially alleviate FasL death signaling from multiple sources and address chronic and tonic signaling issues in engineered T cells.

In addition to FasL signaling, several other inhibitory mechanisms exist in the TME, including immunosuppressive ligand up-regulation, limited antigen presentation, and reduced T cell infiltration into target tissues (Anderson et al., 2017). In our studies, Fas-4-1BB T cells exhibited increased responsiveness to low-level stimulation, increasing proliferation and accumulation. Fas-4-1BB TCR_{gag} T cells exhibited enhanced function in response to FBL cells despite concurrent tumor PD-L1 expression. Fas-4-1BB expression can also overcome tumor trafficking obstacles; IHC revealed higher TIL concentrations and Fas-4-1BB T cells exhibited significantly enhanced accumulation (versus TCR-only T cells) in a competitive cotransfer experiment. Another potential barrier to therapeutic T cell function is the limited availability of metabolic substrates in the TME (Buck et al., 2017; Delgoffe, 2016; Kishton et al., 2017); TIL increasingly lose mitochondrial generation and metabolic efficiency, which is not restored by PD-1 blockade (Menk et al., 2018). However, the addition of 4-1BB costimulation, either within the context of a CAR (Kawalekar et al., 2016) or with anti–4-1BB antibody stimulation (Menk et al., 2018; Teijeira et al., 2018), can increase metabolic capacity and immunotherapeutic T cell efficacy. We have now shown that IFP-engineered T cells also exhibit enhanced mitochondrial biogenesis and metabolic reprogramming in vitro and higher in vivo persistence in ACT against both liquid and solid tumors.

Taken together, our results show that expression of a Fas-4-1BB IFP in tumor-specific T cells produces several enhancements to antitumor T cell function, yielding a high return for minimal manipulation. We provide strong evidence that intentionally engineered IFPs can significantly improve ACT efficacy across multiple cancer types, further supporting clinical translation.

Materials and methods

Generation of murine constructs and retroviral transduction

DNA constructs were ordered from Invitrogen or generated in-house by PCR. The constructs were directionally TOPO cloned into the pENTR/D-TOPO vector and then transferred to the pMP71-attR RV using Gateway technology. The Plat-E (Cell-Bio Labs) RV packaging cell line was transfected using the effectene reagent (Qiagen). Viral supernatant was collected 2 and 3 d later. 1 d before transduction, splenocytes were stimulated with anti-CD3/CD28 and 100 U/ml recombinant human IL-2 (Prometheus). Transduction was performed over 2 d by daily spinfection in 12-well plates with polybrene for 90 min at 1,000×*g*. Engineered T cells were maintained in culture with IL-2 supplementation every 2 d (50 IU/ml) and were restimulated/expanded with either irradiated splenocytes (5×10^6), irradiated FBL (3×10^6), and IL-2 (50 IU/ml) for TCR_{gag} T cells or $peptide_{gp33}$-pulsed irradiated splenocytes and IL-2 (50 IU/ml) for P14 T cells.

Adoptive immunotherapy of disseminated FBL

The B6 (FBL) is a transplantable murine leukemia cell line that expresses an immunogenic peptide derived from the retroviral Gag protein and is used to model disseminated leukemia (Teague et al., 2006). TCR_{gag} transgenic mice express a TCR in CD8 T cells that is specific for the Friend virus gag epitope, peptide CCLCLTVFL (Öhlén et al., 2002). For in vivo FBL studies, B6 mice were injected with 4×10^6 FBL cells i.p. After allowing 5 d, during which FBL disseminates widely, mice received 180 mg/kg Cy i.p. for >6 h to allow drug clearance before transfer of the effector T cells. For survival studies, 10^6 TCR_{gag} T cells that had been previously stimulated twice in vitro were transferred into

tumor-bearing mice. Mice were regularly monitored for increasing tumor burden and euthanized if evidence of tumor progression predicted mortality would occur within 24–48 h. Transferred T cells were analyzed via retro-orbital bleeds to analyze their persistence and phenotype. Short-term survival studies were performed similarly, and mice were euthanized for analysis on the indicated days after T cell transfer.

KPC mice model and adoptive T cell immunotherapy

From 8 wk of age, KPC mice were monitored weekly by high-resolution ultrasound imaging (Vevo 2100) and enrolled in the study upon autochthonous tumor development (≥3 mm mass on the pancreas). Mice were assigned to treatment groups using a random number generator (https://www.random.org). Enrolled mice were treated with Cy (180 mg/kg) and received 10^7 twice-stimulated engineered T cells (i.p.), followed by an infusion of 10^7 peptide$_{Msln}$-pulsed irradiated splenocytes as a tumor antigen vaccine. Short-term study mice were euthanized at day 28 after transfer of a single dose of T cells. Survival study mice received two additional transfers of T cells/splenocytes without Cy pretreatment, for a total of three infusions. The mice were tested for T cell persistence via retro-orbital bleeds. In separate studies, P14 T cells transduced with TCR$_{Msln}$ or TCR$_{Msln}$/Fas-4-1BB were combined at a 1:1 ratio and i.p. injected. Mice were euthanized at day 28 and TIL analyzed by flow cytometry.

Experimental animals and cell lines

C57BL/6 (B6) recipient mice were purchased from The Jackson Laboratory. All animal studies were approved under University of Washington (#2013-01) or Fred Hutchinson Cancer Research Center (#50937) Institutional Animal Care and Use Committees. The genetic backgrounds of P14 and TCR$_{gag}$ mice were assessed at the DartMouse Speed Congenic Core Facility at the Geisel School of Medicine at Dartmouth. DartMouse uses the Illumina Infinium Genotyping Assay to interrogate a custom panel of 5,307 single nucleotide polymorphisms (SNPs) spread throughout the genome. The raw SNP data were analyzed using DartMouse's SNaP-Map and Map-Synth software, allowing the determination for each mouse of the genetic background at each SNP location. Genetic background was determined to be >96.2% for P14 and >98.7% for TCR$_{gag}$ for the desired C57BL/6J background. Cell lines were routinely screened for mycoplasma in the Fred Hutchinson Cancer Research Center testing core.

Flow cytometry reagents

Fluorophore-conjugated murine antibodies were purchased from eBioscience, including antibodies specific for CD8a (53–6.7; catalog #48-0081-80), Thy1.1 (HIS 51; 25-0900-82), Tim3 (RMT3-23; 14–5870-81), Lag3 (ebioC9B7W; 12–2231-81), CD137 (17B5; 17-1370-80), KLRG1 (2F1; 175893–81), and CD25 (PC 61.5; 17–0251-81). Other antibodies to FasL (K10; 106805), vβ9 (MR10-2; 553201), CD69 (H1.2F3; 104502), CD127 (A7R34; 135013), CD80 (16-10A1; 553768), CD86 (GL-1; 105011), IL-2 (JES6-5H4; 503807), IFNγ (XMG1.2; 505809), TNFα (Mab11; 502913), Bax (6A7; 633801), and Bcl-2 (10C4; 633507) were purchased from Biolegend. 7AAD (A1310) and other antibodies were purchased from BD Biosciences, including Fas (Jo2; 563647), Thy1.2 (53–2.1; 561616), CD103 (M290; 557495), purified rat anti-mouse CD16/CD32 (2.4G2; 12–4875-80), PD-1 (J43; 11–9985-81), and Vβ8.1/8.2 (553185). Antibodies against pAKT (S473; D9E; 5315S) were purchased from Cell Signaling Technology. Anti-Eomes (DAN11 mag; 12–4875-80) and the LIVE/DEAD Fixable Aqua Dead Cell Stain Kit (L34957) were purchased from ThermoFisher. For FasL detection, Panc1 cells were treated for 24 h with 3 µg/ml Batimastat (BB-94; ab146619) purchased from Abcam. Flow cytometry data were acquired on a BD FACS Canto II instrument or LSR II and analyzed with Flowjo v9 software.

Isolation of mononuclear cells from murine tissues

Mechanical force was applied to disrupt the spleen, and splenocytes were forced through a 70-µm cell strainer nylon mesh (Falcon). Isolated splenocytes were centrifuged at 369×*g* for 5 min and then treated with activated Cdc42-associated kinase lysis buffer (ThermoFisher) to remove red blood cells. Tumors and lymph nodes excised from FBL mice were disrupted using mechanical force and then processed similarly. Pancreatic tumors retrieved from KPC mice were minced and incubated for 30 min in 1 mg/ml collagenase (Sigma) at 37°C, washed in T cell media, and strained through 70-µm cell strainer nylon mesh (Falcon).

Intracellular cytokine production assay

10^5 of transduced TCR$_{gag}$ T cells were stimulated in vitro with serially diluted tumor cells for 4–6 h in the presence of GolgiPlug (Biolegend). Cells were then stained with the LIVE/DEAD Fixable Aqua Dead Cell Stain (ThermoFisher), followed by the Cytofix/Cytoperm kit (BD Biosciences) and flow cytometry antibodies. Transduced P14 T cells were stimulated with 1 µg/ml of peptide (LCMV$_{gp33-41}$, ELIM peptide) and then cultured, fixed, and stained as described above. In some experiments, anti-Fas (Jo2) antibody (200 ng/ml) or anti-FasL (Kay-10) antibody (150 ng/ml) was added.

T cell proliferation assay

10^5 of transduced TCR$_{gag}$ T cells were labeled using the Cell Trace Violet Cell Proliferation Kit (ThermoFisher) and stimulated in vitro with FBL for 6 d. In separate studies, transduced P14 T cells were labeled with 10 µM Pacific blue succinimidyl ester (PBSE; 65–0842, Invitrogen) and stimulated at a 1:1 ratio with 1 µg/ml LCMV$_{gp33-41}$ peptide-pulsed irradiated nonpulsed splenocytes or anti-Fas (Jo2) antibody (200 ng/ml). In some experiments, anti-Fas (Jo2; 200 ng/ml) or anti-FasL (Kay-10; 150 ng/ml) antibodies were added. On day 6 of the assay, cells were stained for various T cell surface markers and analyzed by flow cytometry.

Caspase-8 assay

0.3 × 10^6 of in vitro stimulated (3×) transduced P14 T cells were stained with 30× FLICA (fluorochrome-labeled inhibitors of caspases) reagent according to the Vybrant FAM Caspase-8 Assay Kit protocol (ThermoFisher). Control Fas$^{-/-}$ splenocytes from TCR$_{Msln}$-transduced *Fas^{lpr}* mice were similarly treated. After FLICA staining, cells were stained with antibodies and analyzed by flow cytometry.

Transcription factor assay

10^5 of previously stimulated TCR_{gag} T cells were stimulated in vitro with 10^5 of target tumor cells (FBL) at a 1:1 ratio for 18–24 h and then stained with ThermoFisher LIVE/DEAD Fixable Aqua, fixed, permeabilized, and stained for intracellular factors according to kit instructions (Foxp3/transcription factor–staining buffer set, eBioscience).

Quantitative PCR

Transduced TCR_{gag} T cells were FACS sorted directly into RLT lysis buffer (supplemented with β–ME) and RNA extracted with the Qiagen RNeasy Plus Mini RNA isolation kit (catalog #74134).

RNA integrity was analyzed on Tape Station analyzer, and cDNA was generated using iScript Reverse Transcription Supermix for quantitative RT-PCR (Biorad; catalog #1708840). Quantitative PCR (qPCR) was run using qPCR SYBR Green Assay with mouse BCL2 PrimePCR assay (Biorad; catalog #10025636) and with RPL13a reference gene (primers: Fwd, 5′-TTCTCCTCCAGAGTGGCTGT-3′, Rev, 5′-GGCTGAAGCCTACCAGAAAG-3′) on the 384-well ABI QuantStudio5 instrument. The ΔΔCT method was used for analysis.

Histology IHC quantification

Harvested tissues were fixed in 10% neutral buffered formalin (3800600, Surgipath) for a minimum of 72 h at room temperature. Fixed tissues were embedded in paraffin, sectioned (4 µm), and stained for hematoxylin and eosin and CD3 (MCA1477, Serotech). Slide scans were analyzed using HALO V2.2.1870.8 software (Indica Labs). Scanned tissue sample areas were determined by manually outlining the tissue, followed by HALO quantification. The number of positively stained cells was determined first by training HALO to identify average intensity and average RGB optical density of 9–25 positive pixels, followed by analyzing consecutive 20× images covering the entire tissue, enumerating positive and negative cells.

Fluorescent microscopy

To visualize Fas localization to the T cell synapse, transduced T cells and FBL tumor cells were combined at a 10:1 ratio, and conjugates were formed by centrifugation (200×*g*), followed by incubation at 37°C for 30 min. 30 µl of cell suspension was added to an Ibidi µ-Slide $VI^{0.4}$ (80606, Ibidi) microscopy slide and incubated at 37°C for 15 min. Cell conjugates were fixed and stained in PBS following the Ibidi staining protocol with Fc Block (553142, BD PharMingen), anti-mouse Fas APC (563647, BD Biosciences), and anti-mouse FasL PE (106805, Biolegend).

To determine mitochondria concentration, MitoTracker Deep Red (M22426, Invitrogen) was resuspended in serum-free RPMI (11875–093, Gibco) to a final concentration of 10 nM (1:100,000) and warmed to 37°C before cells were resuspended in the solution at 10^6 cells/ml and incubated at 37°C for 30 min. Cells were resuspended in PBS and stained in Ibidi µ-Slide $VI^{0.4}$ (80606, Ibidi) as described above, with Fc Block (553142, BD PharMingen), Hoechst (33342, ThermoFisher), and cholera toxin subunit B AF594 (C34777, Life Technologies). All fluorescent microscopy was performed using a DeltaVision Elite high-resolution microscope (GE Healthcare Life Sciences). Captured images were analyzed with ImageJ (National Institutes of Health).

Metabolic analysis using Seahorse

All metabolic assays were conducted using a Seahorse XFe96 Analyzer (Agilent Technologies). Seahorse XFe96 Extracellular Flux Assay Kits (102416–100, Agilent Technologies) were hydrated overnight in 200 µl of double-distilled water (ddH_2O). The ddH_2O was then replaced with 200 µl of 37°C Seahorse XF Calibrant (S5761-500, Agilent Technologies). Cell-Tak (354240, Corning) was activated using sodium bicarbonate (S5761, Sigma-Aldrich) and 1N sodium hydroxide (S2770, Sigma-Aldrich), in accordance with the manufacturer's instructions, before coating Seahorse XF96 cell culture microplates (S2770, Agilent Technologies) with 20 µl/well of 22.4 µg/ml. Cell culture microplates were then left at room temperature for 20 min before being washed twice with 100 µl ddH_2O and air dried for 20 min. Complete assay media was prepared using Seahorse XF base medium (no phenol red; 103335–100, Agilent Technologies) supplemented with 1 mM pyruvate (S8636, Sigma-Aldrich), 2 mM L-glutamine (25030081, Gibco), and 10 mM glucose (G8769, Sigma-Aldrich). Assay media were warmed to 37°C before adjusting the pH to 7.4 using 1N sodium hydroxide (S2770, Sigma-Aldrich) and filtering with a sterile 0.22-µm filter (SLGC033RS, Millex). T cells were resuspended in complete assay media and prewarmed to 37°C at a concentration of 1.38 × 10^6 cells/ml (2.5 × 10^5 cells/180 µl) before plating on a coated cell culture microplate at 180 µl/well and centrifuging the plate at 1,000×*g* for 5 min at 21°C with zero brake. An even coating of cells was confirmed visually before the cell culture plate was transferred to a 37°C non-CO_2 incubator for 0.75 h to ensure cell adhesion. During cell culture plate incubation, the hydrated Seahorse XFe96 Extracellular Flux Assay Kit was loaded with 25 µl of 8-µM oligomycin, 4.5-µM or 13.5-µM carbonyl cyanide-4 (trifluoromethoxy) phenylhydrazone (FCCP), and 5-µM rotenone/antimycin A (XF Cell Mito Stress Test Kit, 103015–100, Agilent Technologies). Final well concentrations were 1-µM oligomycin, 1.5-µM FCCP mitochondrial oxidative phosphorylation uncoupler, and 0.5-µM rotenone/antimycin A. Cellular OCR and extracellular acidification rate were measured under basal conditions and following treatments with oligomycin, FCCP, and rotenone using the Mito Stress Test template available on Wave (Agilent Technologies). Assay results were analyzed using GraphPad Prism.

IncuCyte assay

The IncuCyte NucLight Red Lentivirus Reagent (Essen Biosciences, 4625) was used to transduce FBL and Panc1 cells using the company's standard infection protocol. Transduced cells were purified and purity confirmed on a BD FACS Aria II flow cytometry instrument. For FBL lysis experiments, FBL cells were suspended in fresh growth media and plated in 48-well plates at 10,000 cells/well, and T cells were added at a 3:1 ratio; additional batches of 10,000 FBL were added every 24 h. For Panc1 lysis experiments, 10,000 tumor cells were plated in 96-well plates and allowed to adhere overnight. T cells were added the following day at a 30:1 ratio. Tumor cell lysis was monitored in the IncuCyte ZOOM or S3 and quantified by the loss of red signal (Total Red Object Integrated Intensity [red calibrated unit/micrometer/image]).

CD80, CD86, and FasL blocking studies

To determine if CD28 signaling is necessary for Fas-4-1BB function, NucLight Red$^+$ FBL were untreated or treated with blocking anti-CD80 (16-10A1; 104710) and -CD86 (GL-1; 105010) Biolegend LEAF antibodies and used to serially stimulate Fas-4-1BB T cells every 24 h for three stimulations. 24 h following the last stimulation, the remaining FBL were quantified by IncuCyte analysis.

Statistical analysis

Figures show representative experiments. Analysis was performed using either representative experiments or pooled data, as indicated. GraphPad Prism was used for statistical analyses.

Online supplemental material

Fig. S1 shows in vitro expression and functional data of Fas-41BB and Fas-CD28 P14 T cells. Figs. S2 and S3 show in vitro and in vivo functional data for Fas-4-1BB, Fas-CD28, trFas, and GFP control TCR_{gag} T cells. Fig. S4 shows ex vivo cytokine production and in vivo safety data and persistence of TCR_{Msln} and TCR_{Msln}/Fas-4-1BB T cells. Fig. S5 shows in vitro functional data comparing TCR_{MSLN}, TCR_{MSLN}/Fastm-4-1BB, and trFas human T cells.

Acknowledgments

The authors would like to thank S. Daman, K. Poljakov, S. Ruskin, A. Tu, C. de Imus, K. Ferolito, J. Vazquez Lopez, E. Jensen, J. Nguyen, M. Burnett, I. Stromnes, T. Schmitt, and the Fred Hutchinson Flow Cytometry Core for technical support. We also thank T. Yamamoto (University of California, San Francisco, San Francisco, CA) for the murine trFas (mFas-ΔDD) plasmid and for technical advice. We are grateful to D. Banker for manuscript assistance; R. Perret, S. Srivastava, and M. McAfee for helpful conversations; and N. Duerkopp, S. Hsu, A. Barnes, and M. Gonzalez-White for administrative support.

This work was supported by National Institutes of Health National Cancer Institute grants (CA018029 and CA033084) to P.D. Greenberg; Leukemia & Lymphoma Society grants to S.K. Oda; an Ovarian Cancer Research Alliance Ann and Sol Schreiber Mentored Investigator Award to K.G. Anderson; and a grant from Juno Therapeutics to P.D. Greenberg.

Author contributions: S.K. Oda, K.G. Anderson, P. Ravikumar, P. Bonson, N.M. Garcia, C.M. Jenkins, E.Y. Chiu, S. Zhuang, B.M. Bates, and A.W. Daman performed experiments and analyzed data. S.K. Oda and P.D. Greenberg designed the study. S.K. Oda, K.G. Anderson, P. Ravikumar, P. Bonson, and P.D. Greenberg wrote the manuscript.

Disclosures: S.K. Oda reported grants from Juno Therapeutics during the conduct of the study. P.D. Greenberg reported grants from Juno Therapeutics and personal fees from Juno Therapeutics during the conduct of the study. P.D. Greenberg reported personal fees from Rapt Therapeutics, personal fees from Elpiscience, personal fees from Celsius, and grants from Lonza outside the submitted work. P.D. Greenberg reported a patent to chimeric receptors pending with Juno Therapeutics. No other disclosures were reported.

Submitted: 25 June 2019
Revised: 2 June 2020
Accepted: 3 August 2020

References

Aktas, E., U.C. Kucuksezer, S. Bilgic, G. Erten, and G. Deniz. 2009. Relationship between CD107a expression and cytotoxic activity. *Cell. Immunol.* 254:149–154. https://doi.org/10.1016/j.cellimm.2008.08.007

Anderson, K.G., I.M. Stromnes, and P.D. Greenberg. 2017. Obstacles Posed by the Tumor Microenvironment to T cell Activity: A Case for Synergistic Therapies. *Cancer Cell.* 31:311–325. https://doi.org/10.1016/j.ccell.2017.02.008

Anderson, K.G., V. Voillet, B.M. Bates, E.Y. Chiu, M.G. Burnett, N.M. Garcia, S.K. Oda, C.B. Morse, I.M. Stromnes, C.W. Drescher, et al. 2019. Engineered Adoptive T-cell Therapy Prolongs Survival in a Preclinical Model of Advanced-Stage Ovarian Cancer. *Cancer Immunol. Res.* 7: 1412–1425. https://doi.org/10.1158/2326-6066.CIR-19-0258

Ankri, C., K. Shamalov, M. Horovitz-Fried, S. Mauer, and C.J. Cohen. 2013. Human T cells engineered to express a programmed death 1/28 costimulatory retargeting molecule display enhanced antitumor activity. *J. Immunol.* 191:4121–4129. https://doi.org/10.4049/jimmunol.1203085

Bartkowiak, T., and M.A. Curran. 2015. 4-1BB Agonists: Multi-Potent Potentiators of Tumor Immunity. *Front. Oncol.* 5:117. https://doi.org/10.3389/fonc.2015.00117

Bera, T.K., and I. Pastan. 2000. Mesothelin is not required for normal mouse development or reproduction. *Mol. Cell. Biol.* 20:2902–2906. https://doi.org/10.1128/MCB.20.8.2902-2906.2000

Binnewies, M., E.W. Roberts, K. Kersten, V. Chan, D.F. Fearon, M. Merad, L.M. Coussens, D.I. Gabrilovich, S. Ostrand-Rosenberg, C.C. Hedrick, et al. 2018. Understanding the tumor immune microenvironment (TIME) for effective therapy. *Nat. Med.* 24:541–550. https://doi.org/10.1038/s41591-018-0014-x

Buck, M.D., R.T. Sowell, S.M. Kaech, and E.L. Pearce. 2017. Metabolic Instruction of Immunity. *Cell.* 169:570–586. https://doi.org/10.1016/j.cell.2017.04.004

Chapuis, A.G., D.N. Egan, M. Bar, T.M. Schmitt, M.S. McAfee, K.G. Paulson, V. Voillet, R. Gottardo, G.B. Ragnarsson, M. Bleakley, et al. 2019. T cell receptor gene therapy targeting WT1 prevents acute myeloid leukemia relapse post-transplant. *Nat. Med.* 25:1064–1072. https://doi.org/10.1038/s41591-019-0472-9

Chen, L., and D.B. Flies. 2013. Molecular mechanisms of T cell co-stimulation and co-inhibition. *Nat. Rev. Immunol.* 13:227–242. https://doi.org/10.1038/nri3405

Choi, B.K., D.Y. Lee, D.G. Lee, Y.H. Kim, S.H. Kim, H.S. Oh, C. Han, and B.S. Kwon. 2017. 4-1BB signaling activates glucose and fatty acid metabolism to enhance CD8$^+$ T cell proliferation. *Cell. Mol. Immunol.* 14:748–757. https://doi.org/10.1038/cmi.2016.02

Contini, P., M.R. Zocchi, I. Pierri, A. Albarello, and A. Poggi. 2007. In vivo apoptosis of CD8(+) lymphocytes in acute myeloid leukemia patients: involvement of soluble HLA-I and Fas ligand. *Leukemia.* 21:253–260. https://doi.org/10.1038/sj.leu.2404494

Curran, M.A., T.L. Geiger, W. Montalvo, M. Kim, S.L. Reiner, A. Al-Shamkhani, J.C. Sun, and J.P. Allison. 2013. Systemic 4-1BB activation induces a novel T cell phenotype driven by high expression of Eomesodermin. *J. Exp. Med.* 210:743–755. https://doi.org/10.1084/jem.20121190

D'Aloia, M.M., I.G. Zizzari, B. Sacchetti, L. Pierelli, and M. Alimandi. 2018. CAR-T cells: the long and winding road to solid tumors. *Cell Death Dis.* 9: 282. https://doi.org/10.1038/s41419-018-0278-6

Delgoffe, G.M.. 2016. Filling the Tank: Keeping Antitumor T Cells Metabolically Fit for the Long Haul. *Cancer Immunol. Res.* 4:1001–1006. https://doi.org/10.1158/2326-6066.CIR-16-0244

Gomes-Silva, D., M. Mukherjee, M. Srinivasan, G. Krenciute, O. Dakhova, Y. Zheng, J.M.S. Cabral, C.M. Rooney, J.S. Orange, M.K. Brenner, et al. 2017. Tonic 4-1BB Costimulation in Chimeric Antigen Receptors Impedes T Cell Survival and Is Vector-Dependent. *Cell Rep.* 21:17–26. https://doi.org/10.1016/j.celrep.2017.09.015

Hassan, R., T. Bera, and I. Pastan. 2004. Mesothelin: a new target for immunotherapy. *Clin. Cancer Res.* 10:3937–3942. https://doi.org/10.1158/1078-0432.CCR-03-0801

Ho, W.Y., H.N. Nguyen, M. Wolfl, J. Kuball, and P.D. Greenberg. 2006. In vitro methods for generating CD8+ T-cell clones for immunotherapy from the naïve repertoire. *J. Immunol. Methods.* 310:40–52. https://doi.org/10.1016/j.jim.2005.11.023

Ichinose, M., J. Masuoka, T. Shiraishi, T. Mineta, and K. Tabuchi. 2001. Fas ligand expression and depletion of T-cell infiltration in astrocytic tumors. *Brain Tumor Pathol*. 18:37–42. https://doi.org/10.1007/BF02478923

Jiang, T., C. Zhou, and S. Ren. 2016. Role of IL-2 in cancer immunotherapy. *OncoImmunology*. 5. e1163462. https://doi.org/10.1080/2162402X.2016.1163462

Kawalekar, O.U., R.S. O' Connor, J.A. Fraietta, L. Guo, S.E. McGettigan, A.D. Posey, Jr., P.R. Patel, S. Guedan, J. Scholler, B. Keith, et al. 2016. Distinct Signaling of Coreceptors Regulates Specific Metabolism Pathways and Impacts Memory Development in CAR T Cells. *Immunity*. 44:712. https://doi.org/10.1016/j.immuni.2016.02.023

Kishton, R.J., M. Sukumar, and N.P. Restifo. 2017. Metabolic Regulation of T Cell Longevity and Function in Tumor Immunotherapy. *Cell Metab*. 26:94–109. https://doi.org/10.1016/j.cmet.2017.06.016

Klinker, M.W., V. Lizzio, T.J. Reed, D.A. Fox, and S.K. Lundy. 2014. Human B Cell-Derived Lymphoblastoid Cell Lines Constitutively Produce Fas Ligand and Secrete MHCII(+)FasL(+) Killer Exosomes. *Front. Immunol*. 5:144. https://doi.org/10.3389/fimmu.2014.00144

Kobold, S., S. Grassmann, M. Chaloupka, C. Lampert, S. Wenk, F. Kraus, M. Rapp, P. Düwell, Y. Zeng, J.C. Schmollinger, et al. 2015. Impact of a New Fusion Receptor on PD-1-Mediated Immunosuppression in Adoptive T Cell Therapy. *J. Natl. Cancer Inst*. 107. djv146. https://doi.org/10.1093/jnci/djv146

Kornmann, M., T. Ishiwata, J. Kleeff, H.G. Beger, and M. Korc. 2000. Fas and Fas-ligand expression in human pancreatic cancer. *Ann. Surg*. 231:368–379. https://doi.org/10.1097/00000658-200003000-00010

Kroon, H.M., Q. Li, S. Teitz-Tennenbaum, J.R. Whitfield, A.M. Noone, and A.E. Chang. 2007. 4-1BB costimulation of effector T cells for adoptive immunotherapy of cancer: involvement of Bcl gene family members. *J. Immunother*. 30:406–416. https://doi.org/10.1097/CJI.0b013e31802eecc6

Künkele, A., A.J. Johnson, L.S. Rolczynski, C.A. Chang, V. Hoglund, K.S. Kelly-Spratt, and M.C. Jensen. 2015. Functional Tuning of CARs Reveals Signaling Threshold above Which CD8+ CTL Antitumor Potency Is Attenuated due to Cell Fas-FasL-Dependent AICD. *Cancer Immunol. Res*. 3:368–379. https://doi.org/10.1158/2326-6066.CIR-14-0200

Laderach, D., M. Movassagh, A. Johnson, R.S. Mittler, and A. Galy. 2002. 4-1BB co-stimulation enhances human CD8(+) T cell priming by augmenting the proliferation and survival of effector CD8(+) T cells. *Int. Immunol*. 14:1155–1167. https://doi.org/10.1093/intimm/dxf080

Lee, D.Y., B.K. Choi, D.G. Lee, Y.H. Kim, C.H. Kim, S.J. Lee, and B.S. Kwon. 2013. 4-1BB signaling activates the t cell factor 1 effector/β-catenin pathway with delayed kinetics via ERK signaling and delayed PI3K/AKT activation to promote the proliferation of CD8+ T Cells. *PLoS One*. 8. e69677. https://doi.org/10.1371/journal.pone.0069677

Lee, J.W., C.A. Komar, F. Bengsch, K. Graham, and G.L. Beatty. 2016. Genetically Engineered Mouse Models of Pancreatic Cancer: The KPC Model (LSL-Kras(G12D/+); LSL-Trp53(R172H/+); Pdx-1-Cre), Its Variants, and Their Application in Immuno-oncology Drug Discovery. *Curr. Protoc. Pharmacol*. 73:14.39.11-14.39.20. https://doi.org/10.1002/cpph.2

Li, H., H. Zhu, C.J. Xu, and J. Yuan. 1998. Cleavage of BID by caspase 8 mediates the mitochondrial damage in the Fas pathway of apoptosis. *Cell*. 94:491–501. https://doi.org/10.1016/S0092-8674(00)81590-1

Liu, X., R. Ranganathan, S. Jiang, C. Fang, J. Sun, S. Kim, K. Newick, A. Lo, C.H. June, Y. Zhao, et al. 2016. A Chimeric Switch-Receptor Targeting PD1 Augments the Efficacy of Second-Generation CAR T Cells in Advanced Solid Tumors. *Cancer Res*. 76:1578–1590. https://doi.org/10.1158/0008-5472.CAN-15-2524

Long, A.H., W.M. Haso, J.F. Shern, K.M. Wanhainen, M. Murgai, M. Ingaramo, J.P. Smith, A.J. Walker, M.E. Kohler, V.R. Venkateshwara, et al. 2015. 4-1BB costimulation ameliorates T cell exhaustion induced by tonic signaling of chimeric antigen receptors. *Nat. Med*. 21:581–590. https://doi.org/10.1038/nm.3838

Martinez, M., and E.K. Moon. 2019. CAR T Cells for Solid Tumors: New Strategies for Finding, Infiltrating, and Surviving in the Tumor Microenvironment. *Front. Immunol*. 10:128. https://doi.org/10.3389/fimmu.2019.00128

Menk, A.V., N.E. Scharping, D.B. Rivadeneira, M.J. Calderon, M.J. Watson, D. Dunstane, S.C. Watkins, and G.M. Delgoffe. 2018. 4-1BB costimulation induces T cell mitochondrial function and biogenesis enabling cancer immunotherapeutic responses. *J. Exp. Med*. 215:1091–1100. https://doi.org/10.1084/jem.20171068

Mills, L.D., L. Zhang, R. Marler, P. Svingen, M.G. Fernandez-Barrena, M. Dave, W. Bamlet, R.R. McWilliams, G.M. Petersen, W. Faubion, et al. 2014. Inactivation of the transcription factor GLI1 accelerates pancreatic cancer progression. *J. Biol. Chem*. 289:16516–16525. https://doi.org/10.1074/jbc.M113.539031

Motz, G.T., S.P. Santoro, L.P. Wang, T. Garrabrant, R.R. Lastra, I.S. Hagemann, P. Lal, M.D. Feldman, F. Benencia, and G. Coukos. 2014. Tumor endothelium FasL establishes a selective immune barrier promoting tolerance in tumors. *Nat. Med*. 20:607–615. https://doi.org/10.1038/nm.3541

Nam, K.O., H. Kang, S.M. Shin, K.H. Cho, B. Kwon, B.S. Kwon, S.J. Kim, and H.W. Lee. 2005. Cross-linking of 4-1BB activates TCR-signaling pathways in CD8+ T lymphocytes. *J. Immunol*. 174:1898–1905. https://doi.org/10.4049/jimmunol.174.4.1898

Nurieva, R.I., S. Chuvpilo, E.D. Wieder, K.B. Elkon, R. Locksley, E. Serfling, and C. Dong. 2007. A costimulation-initiated signaling pathway regulates NFATc1 transcription in T lymphocytes. *J. Immunol*. 179:1096–1103. https://doi.org/10.4049/jimmunol.179.2.1096

Oda, S.K., A.W. Daman, N.M. Garcia, F. Wagener, T.M. Schmitt, X. Tan, A.G. Chapuis, and P.D. Greenberg. 2017. A CD200R-CD28 fusion protein appropriates an inhibitory signal to enhance T-cell function and therapy of murine leukemia. *Blood*. 130:2410–2419. https://doi.org/10.1182/blood-2017-04-777052

Öhlén, C., M. Kalos, L.E. Cheng, A.C. Shur, D.J. Hong, B.D. Carson, N.C. Kokot, C.G. Lerner, B.D. Sather, E.S. Huseby, et al. 2002. CD8(+) T cell tolerance to a tumor-associated antigen is maintained at the level of expansion rather than effector function. *J. Exp. Med*. 195:1407–1418. https://doi.org/10.1084/jem.20011063

Peter, M.E., A. Hadji, A.E. Murmann, S. Brockway, W. Putzbach, A. Pattanayak, and P. Ceppi. 2015. The role of CD95 and CD95 ligand in cancer. *Cell Death Differ*. 22:885–886. https://doi.org/10.1038/cdd.2015.25

Poulaki, V., C.S. Mitsiades, and N. Mitsiades. 2001. The role of Fas and FasL as mediators of anticancer chemotherapy. *Drug Resist. Updat*. 4:233–242. https://doi.org/10.1054/drup.2001.0210

Prosser, M.E., C.E. Brown, A.F. Shami, S.J. Forman, and M.C. Jensen. 2012. Tumor PD-L1 co-stimulates primary human CD8(+) cytotoxic T cells modified to express a PD1:CD28 chimeric receptor. *Mol. Immunol*. 51:263–272. https://doi.org/10.1016/j.molimm.2012.03.023

Ribas, A., and J.D. Wolchok. 2018. Cancer immunotherapy using checkpoint blockade. *Science*. 359:1350–1355. https://doi.org/10.1126/science.aar4060

Roth, T.L., P.J. Li, F. Blaeschke, J.F. Nies, R. Apathy, C. Mowery, R. Yu, M.L.T. Nguyen, Y. Lee, A. Truong, et al. 2020. Pooled Knockin Targeting for Genome Engineering of Cellular Immunotherapies. *Cell*. 181:728–744.e21. https://doi.org/10.1016/j.cell.2020.03.039

Sanchez-Paulete, A.R., S. Labiano, M.E. Rodriguez-Ruiz, A. Azpilikueta, I. Etxeberria, E. Bolaños, V. Lang, M. Rodriguez, M.A. Aznar, M. Jure-Kunkel, et al. 2016. Deciphering CD137 (4-1BB) signaling in T-cell costimulation for translation into successful cancer immunotherapy. *Eur. J. Immunol*. 46:513–522. https://doi.org/10.1002/eji.201445388

Schlenker, R., L.F. Olguín-Contreras, M. Leisegang, J. Schnappinger, A. Disovic, S. Rühland, P.J. Nelson, H. Leonhardt, H. Harz, S. Wilde, et al. 2017. Chimeric PD-1:28 Receptor Upgrades Low-Avidity T cells and Restores Effector Function of Tumor-Infiltrating Lymphocytes for Adoptive Cell Therapy. *Cancer Res*. 77:3577–3590. https://doi.org/10.1158/0008-5472.CAN-16-1922

Seedhom, M.O., H.D. Hickman, J. Wei, A. David, and J.W. Yewdell. 2016. Protein Translation Activity: A New Measure of Host Immune Cell Activation. *J. Immunol*. 197:1498–1506. https://doi.org/10.4049/jimmunol.1600088

Stephan, M.T., V. Ponomarev, R.J. Brentjens, A.H. Chang, K.V. Dobrenkov, G. Heller, and M. Sadelain. 2007. T cell-encoded CD80 and 4-1BBL induce auto- and transcostimulation, resulting in potent tumor rejection. *Nat. Med*. 13:1440–1449. https://doi.org/10.1038/nm1676

Stromnes, I.M., J.N. Blattman, X. Tan, S. Jeevanjee, H. Gu, and P.D. Greenberg. 2010. Abrogating Cbl-b in effector CD8(+) T cells improves the efficacy of adoptive therapy of leukemia in mice. *J. Clin. Invest*. 120:3722–3734. https://doi.org/10.1172/JCI41991

Stromnes, I.M., T.M. Schmitt, A. Hulbert, J.S. Brockenbrough, H. Nguyen, C. Cuevas, A.M. Dotson, X. Tan, J.L. Hotes, P.D. Greenberg, et al. 2015. T Cells Engineered against a Native Antigen Can Surmount Immunologic and Physical Barriers to Treat Pancreatic Ductal Adenocarcinoma. *Cancer Cell*. 28:638–652. https://doi.org/10.1016/j.ccell.2015.09.022

Teague, R.M., B.D. Sather, J.A. Sacks, M.Z. Huang, M.L. Dossett, J. Morimoto, X. Tan, S.E. Sutton, M.P. Cooke, C. Ohlén, et al. 2006. Interleukin-15 rescues tolerant CD8+ T cells for use in adoptive immunotherapy of established tumors. *Nat. Med*. 12:335–341. https://doi.org/10.1038/nm1359

Teijeira, A., S. Labiano, S. Garasa, I. Etxeberria, E. Santamaría, A. Rouzaut, M. Enamorado, A. Azpilikueta, S. Inoges, E. Bolaños, et al. 2018. Mitochondrial Morphological and Functional Reprogramming Following CD137 (4-1BB) Costimulation. *Cancer Immunol. Res.* 6:798–811. https://doi.org/10.1158/2326-6066.CIR-17-0767

Thome, M., and J. Tschopp. 2001. Regulation of lymphocyte proliferation and death by FLIP. *Nat. Rev. Immunol.* 1:50–58. https://doi.org/10.1038/35095508

Thommen, D.S., and T.N. Schumacher. 2018. T Cell Dysfunction in Cancer. *Cancer Cell.* 33:547–562. https://doi.org/10.1016/j.ccell.2018.03.012

van der Windt, G.J., B. Everts, C.H. Chang, J.D. Curtis, T.C. Freitas, E. Amiel, E.J. Pearce, and E.L. Pearce. 2012. Mitochondrial respiratory capacity is a critical regulator of CD8+ T cell memory development. *Immunity*. 36: 68–78. https://doi.org/10.1016/j.immuni.2011.12.007

Vekemans, K., L. Rosseel, E. Wisse, and F. Braet. 2004. Immuno-localization of Fas and FasL in rat hepatic endothelial cells: influence of different fixation protocols. *Micron*. 35:303–306. https://doi.org/10.1016/j.micron.2003.09.001

Villa-Morales, M., and J. Fernández-Piqueras. 2012. Targeting the Fas/FasL signaling pathway in cancer therapy. *Expert Opin. Ther. Targets*. 16: 85–101. https://doi.org/10.1517/14728222.2011.628937

Watanabe-Fukunaga, R., C.I. Brannan, N.G. Copeland, N.A. Jenkins, and S. Nagata. 1992. Lymphoproliferation disorder in mice explained by defects in Fas antigen that mediates apoptosis. *Nature*. 356:314–317. https://doi.org/10.1038/356314a0

Wyzgol, A., N. Müller, A. Fick, S. Munkel, G.U. Grigoleit, K. Pfizenmaier, and H. Wajant. 2009. Trimer stabilization, oligomerization, and antibody-mediated cell surface immobilization improve the activity of soluble trimers of CD27L, CD40L, 41BBL, and glucocorticoid-induced TNF receptor ligand. *J. Immunol.* 183:1851–1861. https://doi.org/10.4049/jimmunol.0802597

Yamamoto, T.N., P.H. Lee, S.K. Vodnala, D. Gurusamy, R.J. Kishton, Z. Yu, A. Eidizadeh, R. Eil, J. Fioravanti, L. Gattinoni, et al. 2019. T cells genetically engineered to overcome death signaling enhance adoptive cancer immunotherapy. *J. Clin. Invest.* 129:1551–1565. https://doi.org/10.1172/JCI121491

Zhu, J., P.F. Petit, and B.J. Van den Eynde. 2019. Apoptosis of tumor-infiltrating T lymphocytes: a new immune checkpoint mechanism. *Cancer Immunol. Immunother*. 68:835–847. https://doi.org/10.1007/s00262-018-2269-y

Supplemental material

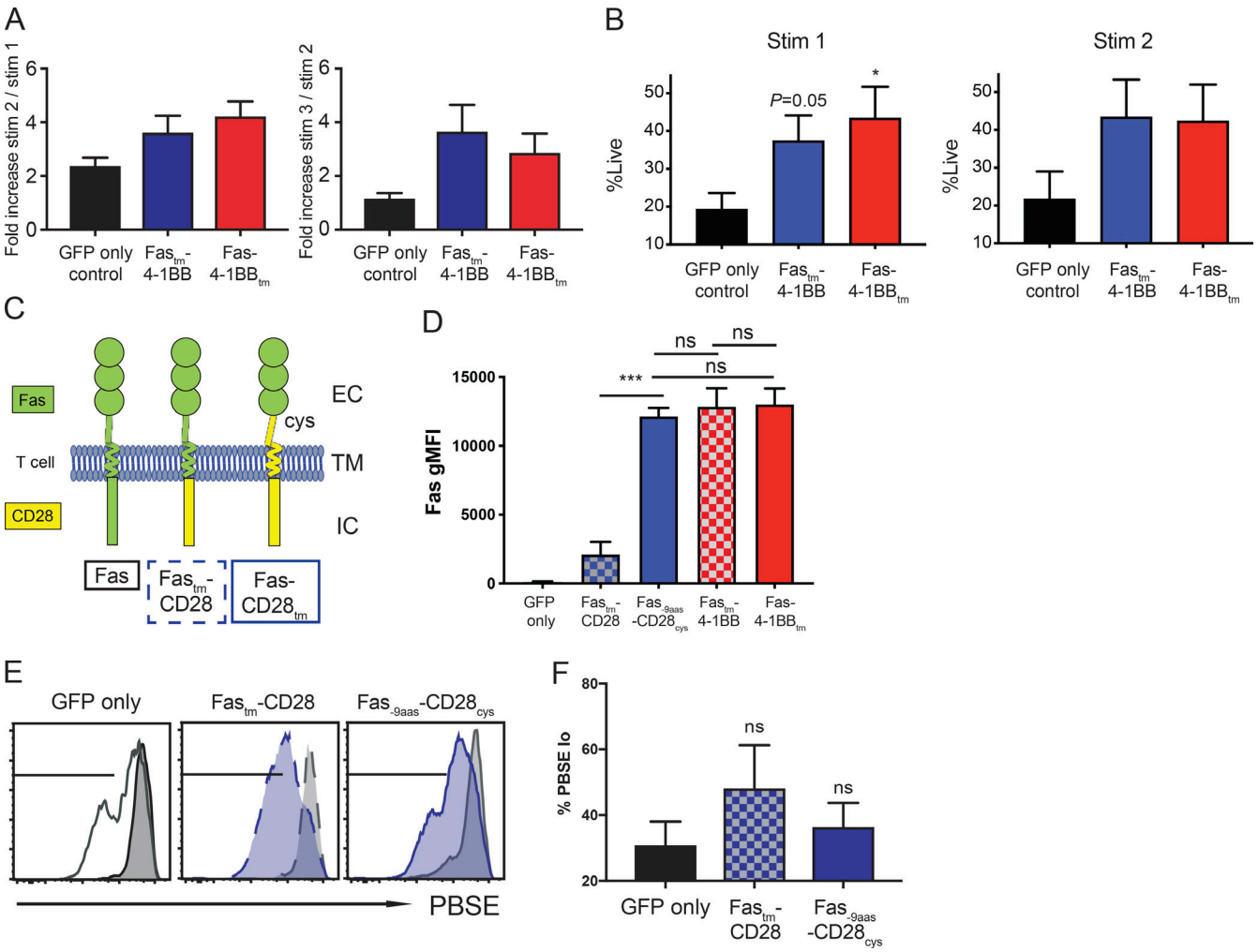

Figure S1. **Engineered P14 T cells were generated as described in Fig. 1. (A)** Enrichment of Fas-4-1BB T cells after in vitro restimulations. A mixed population of transduced (GFP^+) and non-transduced (GFP^-) P14 T cells were restimulated with irradiated $peptide_{gp33}$-pulsed splenocytes and the proportion of GFP^+ P14 T cells quantified by flow cytometry. P = not significant. **(B)** Viability of GFP^+ transduced cells after one or two stimulations as determined by flow cytometry. **(C)** Schematic representation of Fas-CD28 IFP constructs. Fas_{tm}-CD28 (dashed blue box) contains Fas extracellular (EC) and transmembrane (TM) domains and a CD28 intracellular (IC) signaling domain. Fas_{-9aas}-$CD28_{cys}$ (solid blue box) incorporates a portion of the extracellular domain of CD28 to the transmembrane-proximal cysteine to promote multimerization and enhance CD28 signaling. To account for the extra nine extracellular amino acids, Fas was truncated by nine membrane-proximal amino acids (Oda et al., 2017). **(D)** Transgenic expression of Fas on TCR_{gag} T cells transduced with GFP alone, or Fas-CD28 or Fas-4-1BB IFPs, as detected by anti-Fas antibody and flow cytometry. gMFI, geometric MFI. **(E)** Proliferation of engineered, PBSE-labeled P14 T cells as assessed by PBSE dilution 7 d after stimulation with $peptide_{gp33}$-pulsed splenocytes (1 µg/ml) relative to unstimulated T cells (gray). **(F)** Quantification of PBSE dilution of IFP-engineered T cells (gated from E). Data are representative of three (E) experiments or represent the mean of three (F), four (A and D), or seven (B) experiments. ns, not significant. *, $P < 0.05$; ***, $P < 0.001$ by *t* test compared with GFP-only control T cells. Error bars indicate SEM.

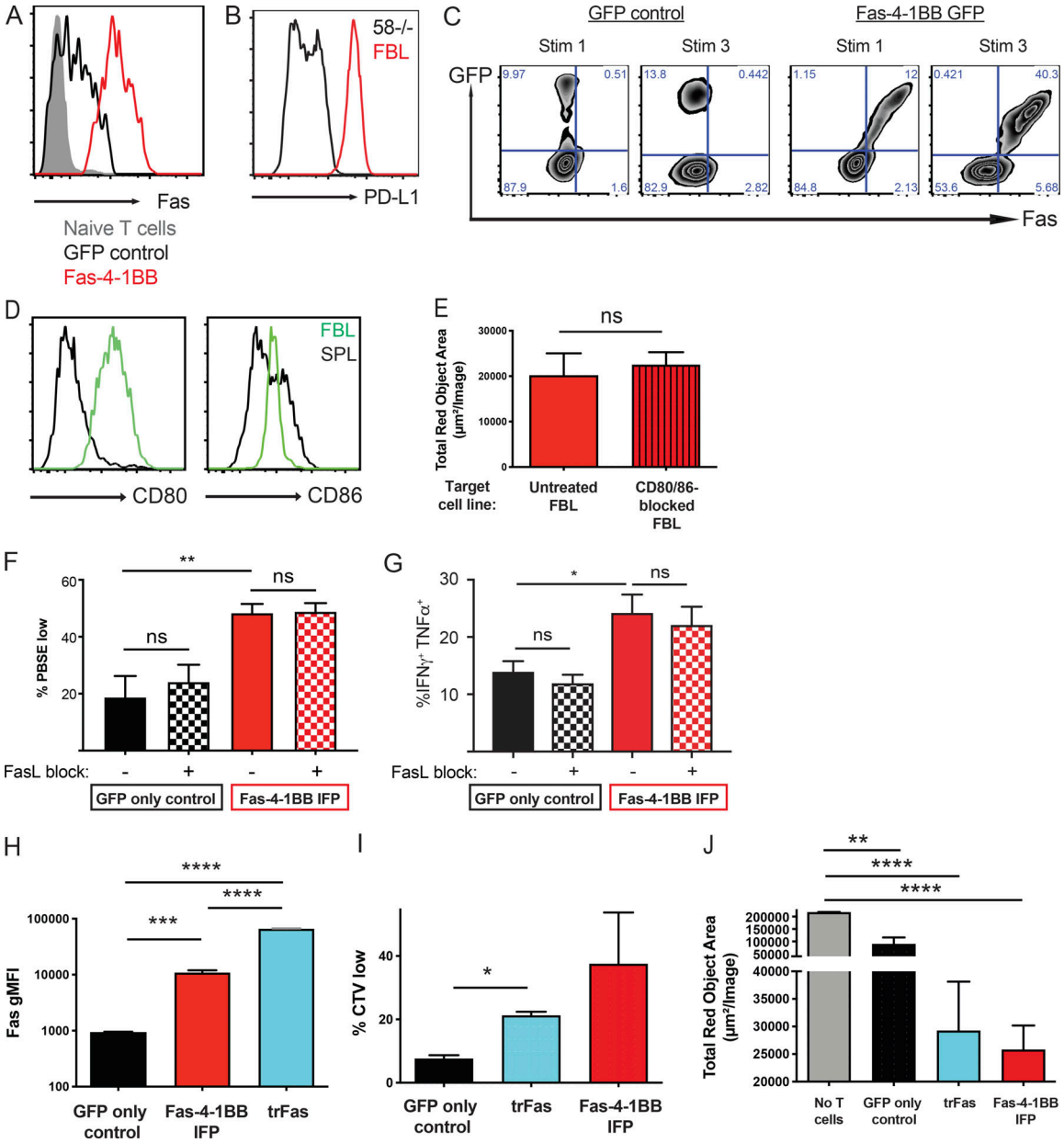

Figure S2. **Fas-4-1BB expression enhances function of transduced T cells.** For A–E, engineered TCR_{gag} T cells were generated as described in Fig. 2. **(A)** Expression of Fas on naïve (gray), GFP-only (black), or Fas-4-1BB with GFP (red) TCR_{gag} T cells as detected by anti-Fas antibody and flow cytometry. **(B)** Expression of PD-L1 on $58^{-/-}$ and FBL murine cell lines as detected by specific antibody staining and flow cytometry. **(C)** Enrichment of Fas-4-1BB T cells after in vitro restimulation. A mixed population of transduced (GFP^+) and non-transduced (GFP^-) TCR_{gag} T cells was restimulated with irradiated $FasL^+$ FBL and splenocytes, and the proportion of GFP^+ TCR_{gag} T cells was quantified by flow cytometry. **(D)** Expression of CD80 and CD86 in FBL (green) and naïve C57BL/6 splenocytes (black) as detected by flow cytometry. SPL, spleen. **(E)** NucLight Red^+ FBL were untreated or treated with blocking anti-CD80 and -CD86 antibodies and used to stimulate Fas-4-1BB–transduced T cells every 24 h for three stimulations. 24 h following the last stimulation, the remaining FBL were quantified by IncuCyte analysis. **(F and G)** Transduced P14 T cells were generated as described in Fig. 1. **(F)** Quantification of PBSE dilution of GFP- or IFP-engineered P14 T cells 7 d after stimulation with $peptide_{gp33}$-pulsed splenocytes with or without FasL-blocking antibody (150 ng/ml). Average of three independent experiments. **, $P < 0.01$; one-way ANOVA for multiple comparisons. **(G)** Cytokine production of engineered P14 T cells after co-culture with $peptide_{gp33}$ (1 µg/ml), with or without blocking anti-FasL antibody (150 ng/ml), for 5 h in the presence of GolgiPlug (BD Biosciences). Culture conditions are indicated below the graph. Cells were fixed, permeabilized, stained for intracellular cytokines, and assessed by flow cytometry. Average of three independent experiments. ns, not significant; *, $P < 0.05$; one-way ANOVA for multiple comparisons. **(H–J)** Engineered TCR_{gag} T cells were generated as described in Fig. 2. **(H)** Geometric MFI (gMFI) of Fas expression in engineered T cells. **(I)** Proliferation of TCR_{gag} T cells (100,000 cells) expressing GFP empty vector control (black), trFas (blue), or Fas-4-1BB (red) as measured by cell trace violet (CTV) dilution by flow cytometry after stimulation with 6,250 FBL for 7 d. **(J)** SKO assay final time point quantification of tumor cells. NucLight Red^+ FBL were co-cultured with TCR_{gag} T cells transduced to express GFP only, trFas, or Fas-4-1BB. NucLight Red^+ FBL were re-added every 24 h for a total of three stimulations/exposures. 24 h following the last stimulation, the remaining FBL were quantified by IncuCyte analysis. Data are representative of two (A–D) experiments or represent the mean of four (E) or three (F–J) experiments. ns, not significant; *, $P < 0.05$; **, $P < 0.01$; ***, $P < 0.001$; ****, $P < 0.0001$; *t* test or one-way ANOVA (H). Error bars indicate SEM. FBL, Friend murine virus (F-MuLV)–induced leukemia.

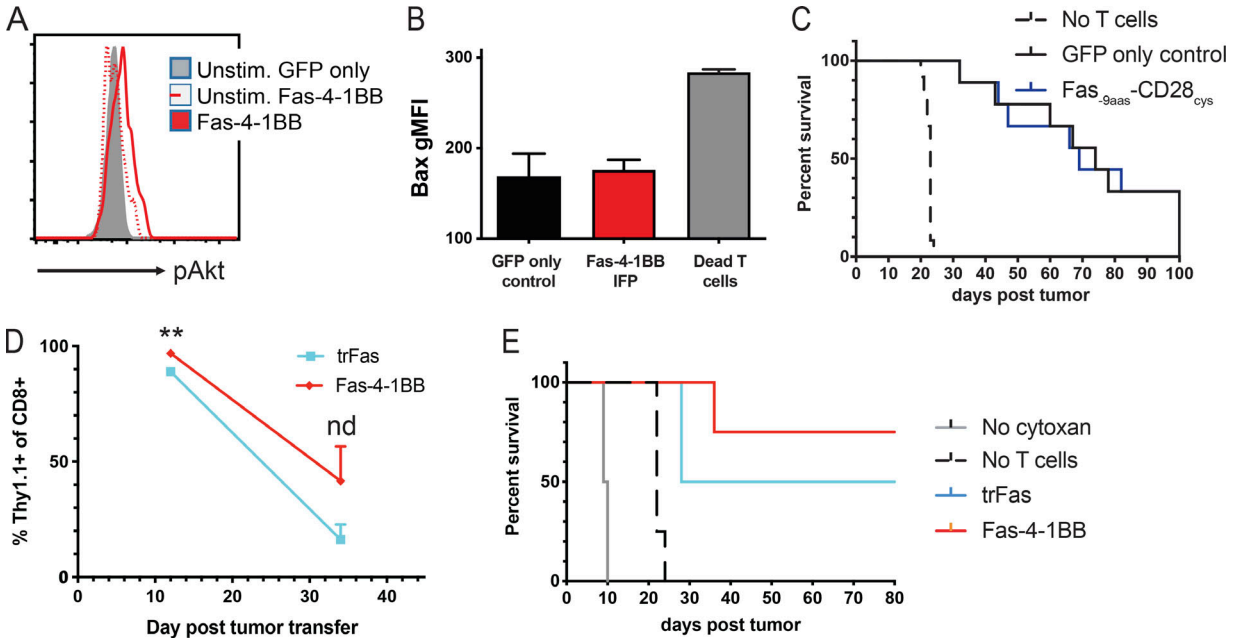

Figure S3. **Transduced TCR_{gag} T cells were generated as described in Fig. 2 and used for in vitro studies (A and B) or ACT (C–E) as described in Fig. 3.** **(A)** Expression of pAkt in engineered T cells. Transduced T cells were incubated overnight alone or with FBL tumor cells at a 1:1 ratio and then were fixed, permeabilized, and stained for intracellular pAKT. Representative of two independent experiments. **(B)** Expression of pro-apoptotic Bax in engineered T cells. Transduced T cells were incubated with FBL tumor cells at a 1:1 ratio overnight and then were fixed, permeabilized, and stained for intracellular Bax and compared with dead T cells as defined by being stained with the viability dye. Average of three studies (GFP versus Fas-4-1BB, P = not significant; *t* test). gMFI, geometric MFI. **(C)** Survival of FBL-bearing mice that received Cy only (n = 12), Cy and GFP control T cells (n = 9), or Cy and Fas_{-9aas}-$CD28_{cys}$ T cells (n = 9). Average of two separate studies (GFP versus Fas_{-9aas}-$CD28_{cys}$, P = not significant; log-rank Mantel-Cox test). **(D)** Persistence of tumor-specific T cells in FBL-bearing mice that received trFas (n = 4) or Fas-4-1BB T cells (n = 4). Mice were bled 12 d and 34 d after tumor transfer, and transferred T cells were detected by flow cytometry of congenic marker expression. At day 12, trFas (n = 4) versus Fas-4-1BB T cells (n = 4): **, P < 0.01; *t* test. At day 34, trFas (n = 2) versus Fas-4-1BB T cells (n = 4): nd (statistics not done, n < 3/group). **(E)** Survival of FBL-bearing mice that received no therapy (n = 2), Cy only (n = 4), Cy and trFas (n = 4), or Cy and Fas-4-1BB T cells (n = 4); trFas versus Fas-4-1BB T cells, P = not significant; log-rank Mantel-Cox test. Error bars indicate SEM.

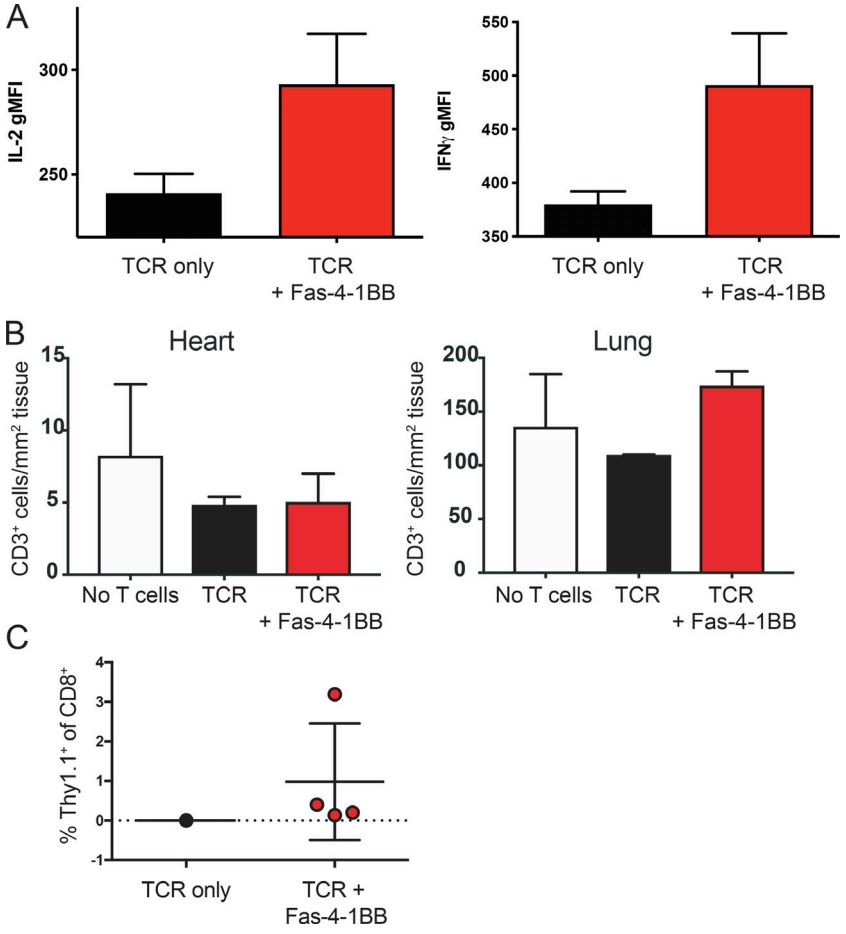

Figure S4. **Fas-4-1BB T cells exhibit greater persistence and do not accumulate in organs that express endogenous Msln. (A and B)** Engineered P14 T cells were generated and transferred to KPC mice as described in Fig. 4. **(A)** Cytokine expression of co-transferred T cells at day 7, as in Fig. 4 E. Tumors were minced and digested with collagenase before incubation with Brefeldin A for 5 h. Samples were then stained for intracellular cytokine expression before evaluation by flow cytometry. *n* = 3; IL-2, P = not significant; IFNγ, P = 0.09; *t* test. **(B)** Tumor-bearing KPC mice received T cells and peptide$_{Msln}$-pulsed splenocytes once after Cy treatment. Mice were euthanized 28 d after transfer, and CD3$^+$ cells were quantified by IHC in KPC lung and heart tissues (*n* = 2/group). P = not significant; one-way ANOVA. **(C)** Persistence of transferred T cells. Mice were treated with three doses of engineered T cells, as in Fig. 4 J. Surviving mice (TCR only, *n* = 1; TCR + Fas-4-1BB, *n* = 4) were bled 28 d after the third T cell transfer, and transferred T cells were detected by flow cytometry of congenic marker expression. gMFI, geometric MFI. Error bars indicate SEM.

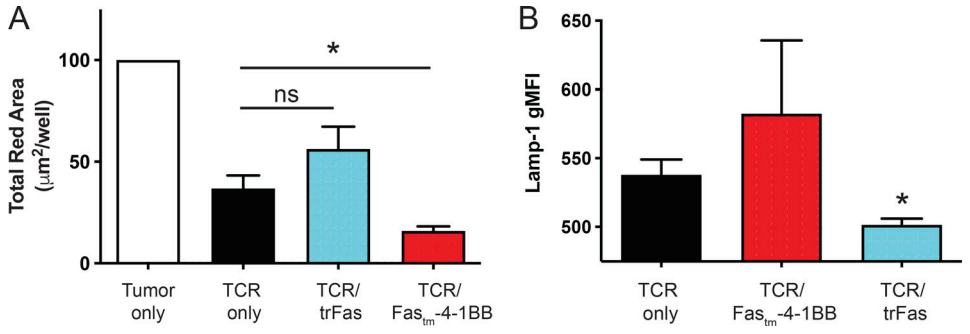

Figure S5. **IncuCyte assay. (A)** NucLight Red$^+$ Panc1 cells were cultured alone (white) or co-cultured with TCR-only (black), TCR/trFas (blue), or TCR/Fas-4-1BB (red) T cells at a 30:1 E:T ratio. Tumor cell concentration was determined by Total Red Area (μm^2/image). Averaged data represent T cells generated from three unique human donors. Statistical analyses are shown: TCR/Fas$_{tm}$-4-1BB versus TCR only, *, P < 0.05; TCR/trFas$_{tm}$-4-1BB versus TCR only, P = not significant; *t* test of final time point. **(B)** Lamp-1 (CD107a) expression of T cells previously exposed to tumor. T cells previously stimulated in the IncuCyte assay (as in A) were restimulated with Panc1 cells for 5 h and then stained for surface and intracellular Lamp-1 (CD107a) before evaluation by flow cytometry. Averaged data represent T cells generated from three unique human donors. TCR only versus TCR/trFas: *, P < 0.05; TCR only versus TCR/Fas$_{tm}$-4-1BB: P = not significant; *t* test. gMFI, geometric MFI.